FULL PAPER

The sequence of the 2017–2018 eruptions and seismo-acoustic activity at Kirishima volcano group

Mie Ichihara[1*] , Tsukasa Kobayashi[2], Fukashi Maeno[1], Takao Ohminato[1], Atsushi Watanabe[1], Setsuya Nakada[3] and Takayuki Kaneko[1]

Abstract

Kirishima volcano consists of more than 20 eruptive centers. Among them, Shinmoe-dake had magmatic eruptions in October 2017 and March 2018. Subsequently, another active cone, Iwo-yama, had phreatic eruptions in April 2018. These events were unique in that the 2018 eruption was the first effusion-dominated eruption of Shinmoe-dake and the first simultaneous activity of two cones of the Kirishima volcanic group ever documented. We report the detailed sequence of the events by combining areal photos, satellite images, and seismo-acoustic data analyses with the other published information. The seismo-acoustic data clarify the eruption onset and the transitions of the behaviors in three stages for each of the 2017 and 2018 eruptions. For both eruptions, we present regularly repeated tremors or 'drumbeat' earthquakes in the second stage, which interpret as gas separation from magma, leading to the ash-poor plume in the 2017 eruption or the effusive eruption in the 2018 event. We also propose that the 2017 and 2018 eruptions of Shinmoe-dake and the 2018 eruption of Iwo-yama are sequential events linked by the degassing of magma beneath Shinmoe-dake. An eruption like the 2017–2018 eruptions of Shinmoe-dake would leave few geological records and could be captured only by modern techniques. Although Shinmoe-dake has been believed to be an example of less-frequent eruptions, effusive eruptions like the 2018 case might have occurred more frequently in the past , but the following eruptions had obscured their records. The timelines summarized in this study will be useful in future studies of Kirishima volcanoes and world equivalences.

Keywords Eruption sequence, Volcanic group, Volcanic tremor, Eruption types, Volcano monitoring
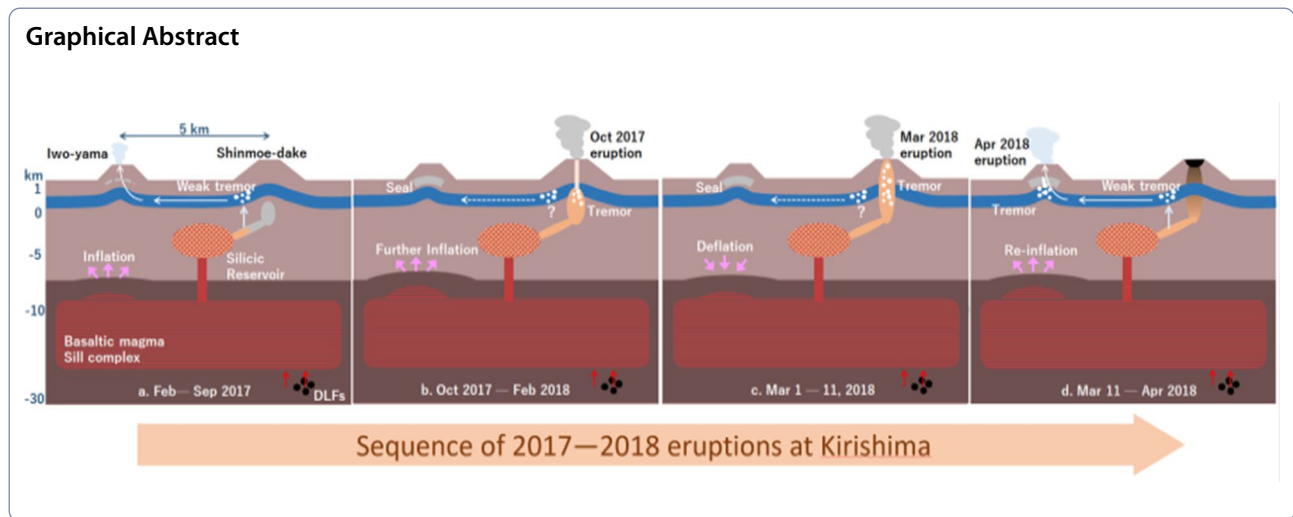
*Correspondence:
Mie Ichihara
ichihara@eri.u-tokyo.ac.jp
Full list of author information is available at the end of the article

Ichihara *et al. Earth, Planets and Space* (2023) 75:144

Page 2 of 21

Graphical Abstract

Introduction

Kirishima volcano, located in southern Kyushu, is one of the most active volcanoes in Japan. The volcano is characterized by having more than 20 eruptive centers distributed along a 30 km northwest–southeast axis and a 20 km northeast–southwest axis (Fig. 1a, b). Each eruption center is characterized by an isolated or near-isolated edifice such as a pyroclastic cone, a strato-volcano, or a maar. Imura (1994) pointed out that many eruptive centers have large craters relative to the edifice volumes, indicating that the eruptions were explosive. In the volcanic group, Shinmoe-dake and Ohachi had magmatic eruptions in the historical periods, and Iwo-yama was born in the sixteenth to seventeenth century (Imura 1994; Imura and Kobayashil 2001; Tajima et al. 2014). Although Ohachi had many magmatic eruptions since the 8th century, Shinmoe-dake and Iwo-yama had only a few historical events before the recent eruptions (Imura 1994; Imura and Kobayashil 2001; Tajima et al. 2014, 2020).

Shinmoe-dake had major magmatic activity in 2011 and 2017–2018. Subsequently, Iwo-yama had phreatic eruptions in 2018. Many studies have already been published for the 2011 event sequences (e.g., Kato and Yamasato 2013; Miyabuchi et al. 2013; Nakada et al. 2013b; Nakao et al. 2013; Ozawa and Kozono 2013; Suzuki et al. 2013a; Takeo et al. 2013; Ueda et al. 2013; Ichihara and Matsumoto 2017), the long-term seismic and geodetic activity including both 2011 and 2018 eruptions (e.g., Kurihara et al. 2019; Yamada et al. 2019; Nishida et al. 2020; Yamazaki et al. 2020; Ichihara et al. 2023), the updated image of magma and fluid supply systems (e.g., Suzuki et al. 2013b; Aizawa et al. 2014; Nagaoka 2020; Ohba et al. 2021; Tajima et al. 2022; Tsukamoto et al. 2022), and the 2018 Iwo-yama eruption sequences (e.g.,

Tajima et al. 2020; Muramatsu et al. 2021). However, the timeline of the 2017–2018 Shinmoe-dake eruption and the transition to the 2018 Iwo-yama eruption have not been sufficiently resolved.

Yamada et al. (2019) reported the chronology of the 2017–2018 Shinmoe-dake eruption based on the multiparametric observation data obtained by the Japan Meteorological Agency (JMA), the National Research Institute for Earth Science and Disaster Resilience (NIED), the Geospatial Information Authority of Japan (GSI), and the Geochemical Research Center of the University of Tokyo. Matsumoto and Geshi (2021) analyzed the frequently collected samples from March 2 to April 5, 2018, and revealed the change of the magma ascent conditions during the 2018 Shinmoe-dake eruption sequence. Tajima et al. (2022) discussed Shinmoe-dake's long-term and recent eruptions (including the 2018 eruption) and its magma plumbing system, based on geological and geophysical observations. Kurihara and Kato (2022) made detailed analyses of the deep low-frequency (DLF) earthquakes and discussed the relationship between their occurrences and the Shinmoe-dake and Iwo-yama activity. We combine their results with our data set to confirm and detail the timeline.

Compared with the previous activity summarized in the next section, the 2017–2018 event was unique for Shinmoe-dake in the following points. First, it was a major magmatic eruption only seven years after the 2011 event. Second, the eruption was dominated by the lava effusion, lacking the sub-Plinian phases. Third, it was the first recorded successive eruptions of two cones in the Kirishima Volcanic Group (Shinmoe-dake and Iwo-yama). Investigating the event will improve our knowledge of Kirishima and other volcanic groups with
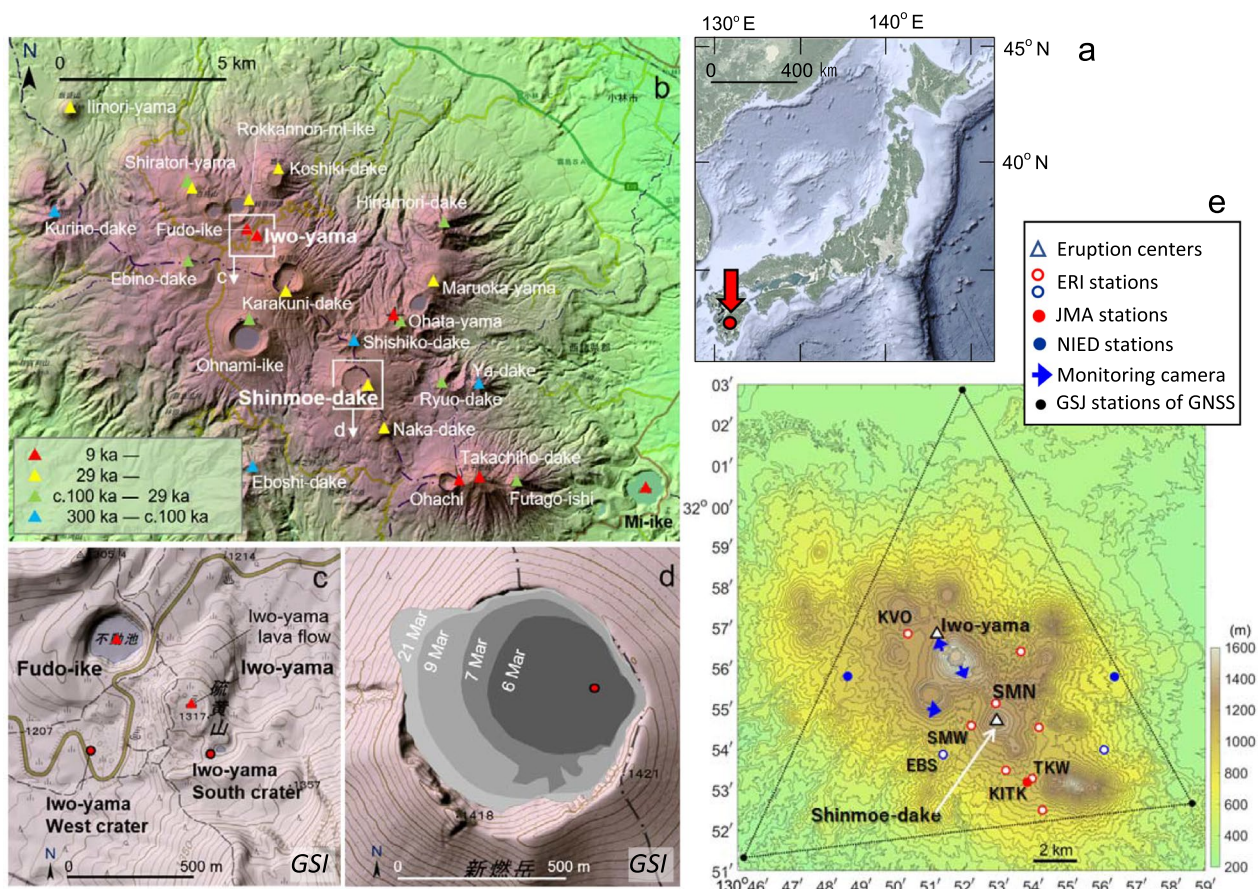
Ichihara *et al. Earth, Planets and Space* (2023) 75:144

Page 3 of 21

Fig. 1 **a** Location of Kirishima volcano. **b** Location of each eruption center of the Younger stage of the Kirishima volcano. Eboshi-dake, Shishiko-dake, Kurino-dake and Ya-dake were formed from 300 ka to ∼100 ka; all of these centers currently have dissected edifices (blue triangles). Shiratori-yama (main), Ebino-dake, Ohnami-ike, Hinamori-dake, Ryuo-dake, Futago-ishi, and Ohata-yama (main) formed from ∼100 ka to 29 ka (green triangles). Maruoka-yama, Iimori-yama, Koshiki-dake, Karakuni-dake, Shinmoe-dake, Shiratori-yama (younger), Rokukannon-mi-ike, and Naka-dake were formed after widespread deposition of the AT (Aira-Tanzawa) tephra at 29 ka (yellow triangles). More recently, Takachiho-dake, Mi-ike (4.2 ka), Ohachi, Ohata-yama (younger), Fudo-ike, and Iwo-yama (AD 1768) were formed after 9 ka (red triangles). Historic records exist for volcanic activity at Shinmoe-dake, Ohachi, and Iwo-yama, which have remained active until the present (Imura and Kobayashi 2001; JMA 2013). **c** Iwo-yama and the surrounding areas. **d** The summit area of Shinmoe-dake. The red circle shows the location of the main eruption in the 2017 activity JMA (2017a). **e** The station locations used in this study. The circles show the seismic stations, of which those used for the tremor source location are colored red.

less-frequent eruptions. The timeline described in this study will help future studies.

Geological overview and eruption activities
Kirishima volcano
Kirishima volcano locates on the southern margin of the Kakuto caldera. The volcano comprises the Younger Kirishima volcano, which forms the present edifices of the Kirishima volcano, and the Older Kirishima volcano, which constitutes the basement of the volcano. Kakuto pyroclastic flow from an eruption of approximately 300 ka is seated between them (Imura 1994; Imura and Kobayashil 2001). The products of the Older Kirishima volcano are composed primarily of andesite, while the

Younger Kirishima volcano has a broad composition, ranging from basalt to dacite (Imura 1994; Imura and Kobayashil 2001). Imura and Kobayashil (2001) divided the eruption centers of the Younger Kirishima volcano into the following four age groups: (1) 300 ka–ca. 100 ka; (2) ca. 100 ka–29 ka; (3) 29 ka–present; and (4) 9 ka–present. The active cones belong to (3) and (4). The distribution of each eruption center is shown in Fig. 1b.

The electromagnetic studies in the 1990s (Utada et al. 1994; Kagiyama et al. 1996, 1997) suggested that the northwestern group, including Shinmoe-dake and Iwo-yama, had a common magma reservoir at a depth of 10 km, from which magma rises to the shallow depth beneath each active volcano. They considered the

Ichihara *et al. Earth, Planets and Space* (2023) 75:144

Page 4 of 21

southeastern group, including Ohachi, to have a separated and even deeper reservoir. Seismological structural studies also showed low-velocity anomalies at a depth of 10–15 km (Yamamoto and Ida 1994; Nagaoka 2020). The three-dimensional electromagnetic analyses resolved a conductive layer at a corresponding depth and conductive pathways to Shinmoe-dake and Iwo-yama (Aizawa et al. 2014).

The existence of a shallow magma reservoir around 5 km was suggested by the petrological studies for the 2011 eruption products (Suzuki et al. 2013b). Based on resistivity studies, Utada et al. (1994) suggested magma storage at ∼5 km bsl beneath Iwo-yama as well as the one beneath Shinmoe-dake, and Aizawa et al. (2014) revealed a sub-vertical conductive body at a depth of ∼ 5 km between Iwo-yama and Shinmoe-dake, which they interpreted as a pathway of magmatic fluid. Yamamoto and Ida (1997) analyzed the P-wave attenuation structure and found a high attenuation at a depth of about 5 km beneath Karakuni-dake. The attenuation was significant for a specific frequency range of around 8 Hz, which the authors explained by a shill-like magma body. However, no movements have been detected at this depth by geophysical methods.

Shinmoe-dake

Shinmoe-dake is at the central, southeastern part of the Kirishima volcano and has a conical edifice that is 1421 m high with a crater measuring 800 m in diameter at the summit (Fig. 1b, d). The basal and upper parts of the edifice are composed of lava flows (Shinmoe-dake lava) and a pyroclastic cone, respectively (Imura and Kobayashil 2001). Kobayashi pumice ejected from Karakuni-dake was deposited on the western slope of Shinmoe-dake, indicating that the main body of Shinmoe-dake formed before 16 ka (Imura 1994; Imura and Kobayashil 2001).

Shinmoe-dake had undergone repeated magmatic eruptions with intervals lasting hundreds to thousands of years (Tajima et al. 2013; Tajima 2021). The first historic event occurred in 1716–1717. The eruption began with phreatic explosions, followed by sub-Plinian eruptions with pyroclastic flows and Vulcanian events. The total mass of tephra was estimated at about 200×10^9 kg (Imura and Kobayashil 1991; Oikawa et al. 2012). Eruptions also occurred in 1822 and 1959. Imura and Kobayashil (1991) estimated that each eruption produced several 10^9 kg of tephra and considered the 1822 event included magmatic activity. They characterized the Shinmoe-dake eruption by the initial phreatic explosions and the transition to explosive magmatic eruptions based on their geological studies of the past magmatic activities (1716–1717 and 1822). Oikawa et al. (2012) reviewed the subsequent studies on Shinmoe-dake's historical eruptions and noted

Table 1 Erupted masses at Shinmoe-dake

Event	Tephra mass (x 10^9 kg)	Lava mass (x 10^9 kg)
2018	< 1	30^a
2017	< 1	–
2011	$18–41^b$	30^c
2008	0.2^d	–
1991–1992	0.00036^d	–
1959	$3–9^{e,f}$	–
1822	$0.3–3^{e,f}$	–
1716–1717	200^f	-

[a] Matsumoto and Geshi (2021); Kozono et al. (2023)
[b] Maeno et al. (2014); Miyabuchi et al. (2013)
[c] Ozawa and Kozono (2013)
[d] Geshi et al. (2010)
[e] Oikawa et al. (2012)
[f] Imura and Kobayashil (1991)

that the 1822 eruption was minor ($< 10^9$ kg of tephra), while the tephra from the 1959 eruption might have been as large as $\sim 9 \times 10^9$ kg and included some juvenile materials. There were minor phreatic eruptions in 1991–1992 and 2008–2010 (Imura 1992; Geshi et al. 2010; Nakada et al. 2013b).

The 2011 eruption at Shinmoe-dake

Inflation of the Kirishima volcano was initially observed from the end of November 2009, centered at a depth of 6–10 km and about 7 km to the northwest of Shinmoe-dake, around the Ebino-dake area of Fig. 1b (Imakiire and Oowaki 2011; Nakao et al. 2013). Small, possibly phreatic eruptions occurred intermittently from March to July 2010 (Kato and Yamasato 2013). Thereafter, inflation of the volcano continued (Kato and Yamasato 2013; Nakao et al. 2013). On January 19, 2011, a small phreatomagmatic eruption occurred (Kato and Yamasato 2013; Suzuki et al. 2013a). Seven days later, on the morning of January 26, the ejection of ash was observed before activity shifted to a sub-Plinian eruption in the afternoon (Nakada et al. 2013b). Three sub-Plinian eruptions occurred until the following evening (Nakada et al. 2013b). On January 28, a tip of effusing lava was observed in the summit crater. The lava flow increased gradually in size over the period January 28–31, finally becoming a circular-shaped lava flow with a diameter of 600 m (Ozawa and Kozono 2013). The summit crater had exhibited a funnel-shaped topography before the 2011 eruption and was half-filled with lava after the event. During the sub-Plinian and effusive stages, the deep geodetic source that had exhibited a-year-long inflation deflated coherently to the magma discharge, confirming the

Ichihara *et al. Earth, Planets and Space* (2023) 75:144

Page 5 of 21

Fig. 2 a Northwesterly view of the Shinmoe-dake summit during the 2017 activity, taken by S. Nakada (14:29, October 11, 2017). **b** Eruption plume of the 2017 Shinmoe-dake eruption viewed from Shinyu hot springs on the southwestern foot of the edifice taken by T. Kaneko (October 12, 2017). **c** Southwesterly view of the summit during the 2018 Shinmoe-dake activity, taken by S. Nakada (shortly before 10:00, March 3, 2018). **d** Northeasterly view of the effusing lava in the Shinmoe-dake summit crater taken by Mainichi Shinbun (5:20, March 6, 2018). **e** Close-up photograph of the effusing lava in the Shinmoe-dake summit crater taken by Mainichi Shinbun (5:17, March 6, 2018). **f** Westerly view of the Shinmoe-dake summit crater taken by S. Nakada (17:26, March 9, 2018). The tip of the northwestern margin of the lava filling the crater is about to flow down the slope (indicated by a yellow allow). **g** Small Vulcanian eruption during the 2018 Shinmoe-dake activity taken from the southwest by S. Nakada (17:30, March 9, 2018). **h** Lava flow flowing down the northwestern slope of Shinmoe-dake, taken by S. Nakada (10:25, April 20, 2018). **i** Shinmoe-dake summit just before the Vulcanian eruption shown in "(**j**)" taken by S. Nakada (10:09, March 10, 2018). The ca. 150 m diameter area near the eruption site swells like a shield. **j** Vulcanian eruption occurred at the site shown in "(**i**)", taken by S. Nakada (10:15, March 10, 2018). **k** Eruption site of the Vulcanian eruptions, located in the central part of the lava flow at the summit, taken by T. Kaneko from the east (March 13, 2018). Yellow arrows indicate pit craters. **l** Eruption site of the Vulcanian eruptions taken by F. Maeno from the west (April 15, 2018). **m** Vulcanian eruption on May 14, 2018, recorded by a JMA monitoring camera. **n** Westerly view of Iwo-yama and surrounding areas taken by JMA (April 21, 2018). **o** Activity of Iwo-yama immediately before the April 19 eruption, recorded by a JMA monitoring camera (15:38, April 19, 2018). **p** The April 19 Iwo-yama eruption recorded by a JMA monitoring camera (15:44, April 19, 2018)

linkage between this source and Shinmoe-dake (Kobayashi et al. 2011; Kozono et al. 2013; Nakao et al. 2013; Ueda et al. 2013). Some researchers suppose that the linkage is only mechanical and that the erupted magma was supplied from the widely spread magma reservoir revealed by the geophysical imaging (Utada et al. 1994; Nagaoka 2020; Nishida et al. 2020; Kurihara and Kato 2022). After January 29, the activity shifted to intermittent explosive eruptions, mainly Vulcanian eruptions, which continued until September of the same year (Kato and Yamasato 2013; Nakada et al. 2013b).

The 2011 event followed Shinmoe-dake's typical eruption sequence that Imura and Kobayashil (1991) had characterized. Namely, it started with phreatic (phreatomagmatic) eruptions and shifted to explosive magmatic phases. Although the previous historical eruptions were dominated by explosive activity (Imura and Kobayashil 1991), the 2011 event erupted lava, whose amount was comparable with the tephra produced by the sub-Plinian events (Ozawa and Kozono 2013; Maeno et al. 2014). Table 1 summarizes the estimated weights of the erupted materials from Shinmoe-dake.
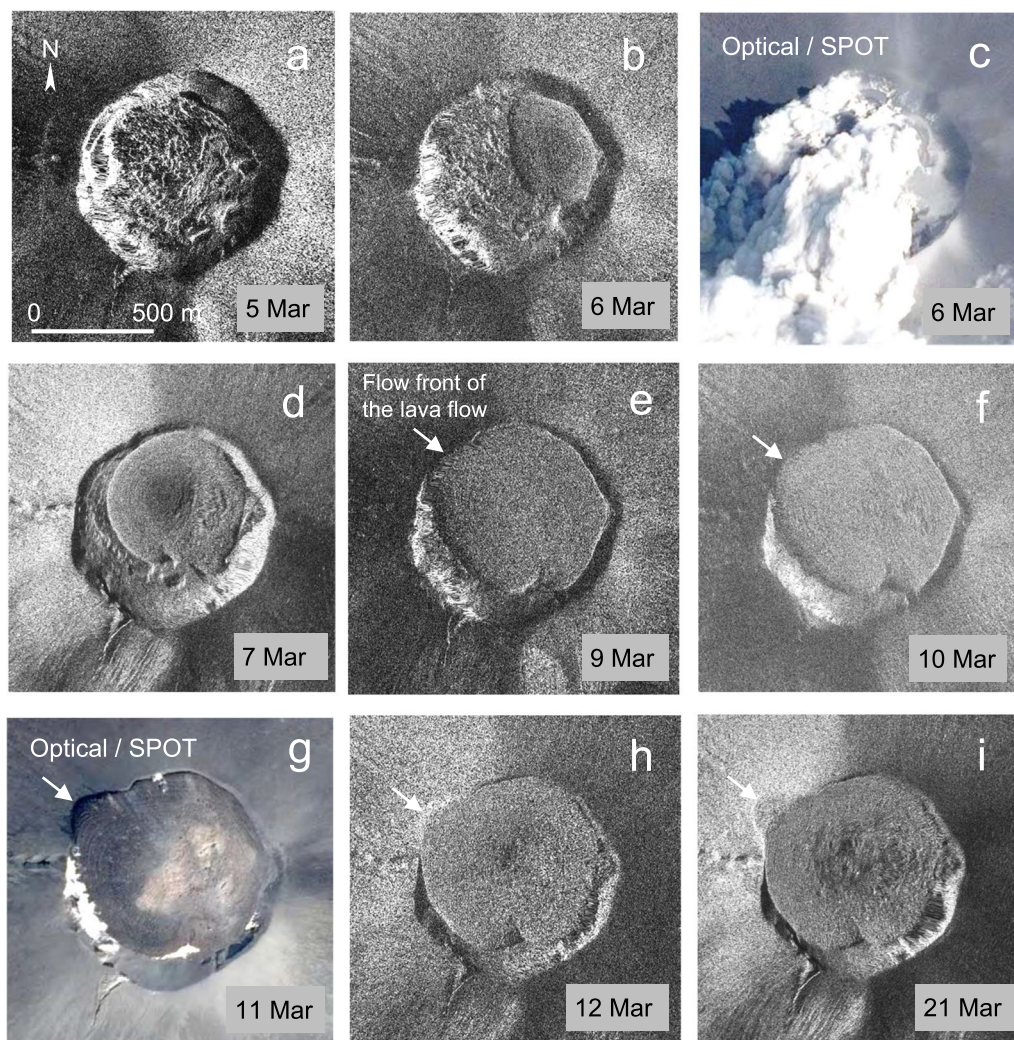
Ichihara *et al. Earth, Planets and Space* (2023) 75:144

Page 6 of 21

Fig. 3 The summit area of Shinmoe-dake observed by the series of satellite images during the 2018 volcanic activity. **a**,**b**, **d**–**f** and **h**–**i** are SAR images from ALOS-2 (Advanced Land Observing Satellite-2 of JAXA—Japan Aerospace Exploration Agency). **c** and **g** are optical images from SPOT 7 (Satellite imagery courtesy of PASCO Corporation: cAirbus DS 2018). Note that the elongated lava shape is artificial, and the lava is more circular, like in Fig. 1d

Iwo-yama

Iwo-yama locates about 5 km northwest of Shinmoedake, on the northwestern foot of the highest cone, Karakunidake (Fig. 1b, c). Eruptions have occurred intermittently in the area since the formation of Karakuni-dake (29 ka). Tajima et al. (2014) summarized the volcanic activity in this area as follows. At 9 ka, eruptions occurred in the Fudo-ike crater, which generated Fd-TmA tephra and Fudo-ike lava flow. Phreatic to phreatomagmatic eruptions occurred at 4.3 ka at the northern part of Karakuni-dake, which ejected Kn-EbD tephra and caused an avalanche of Karakuni-dake debris. At 1.6 ka, phreatic eruptions occurred at the Fudo-ike crater, ejecting Fd-EbC tephra. In the sixteenth to seventh centuries, eruptions in the area generated Io-EbB tephra and Iwo-yama lava flow. Iwo-yama is a small lava mound (∼50 m relative height) formed around the effusion vent. In 1768, phreatic explosions occurred at the eastern crater of Iwo-yama, which ejected Ie-EbA tephra. Geothermal activity is known to have continued there since around the 1900s. The fumarolic activity exhibited the highest temperature in 1975, but gradually declined to have stopped by 2008 (Tajima et al. 2020).
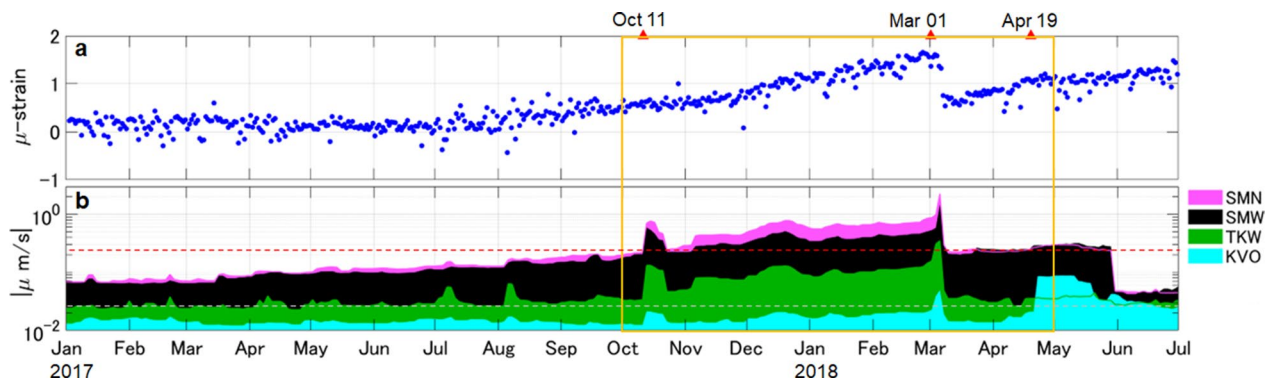
Ichihara *et al. Earth, Planets and Space* (2023) 75:144

Page 7 of 21

Fig. 4 a The areal strain calculated from the three GNSS stations shown in Fig. 1e (Nishida et al. 2020). **b** The seismic background level at 3.5–7 Hz (Ichihara et al. 2023) for four stations as in the legend. The red triangles indicate the onsets of the 2017 and 2018 eruptions of Shinmoe-dake and the 2018 eruption of Iwo-yama. The yellow rectangle period is shown in Fig. 5
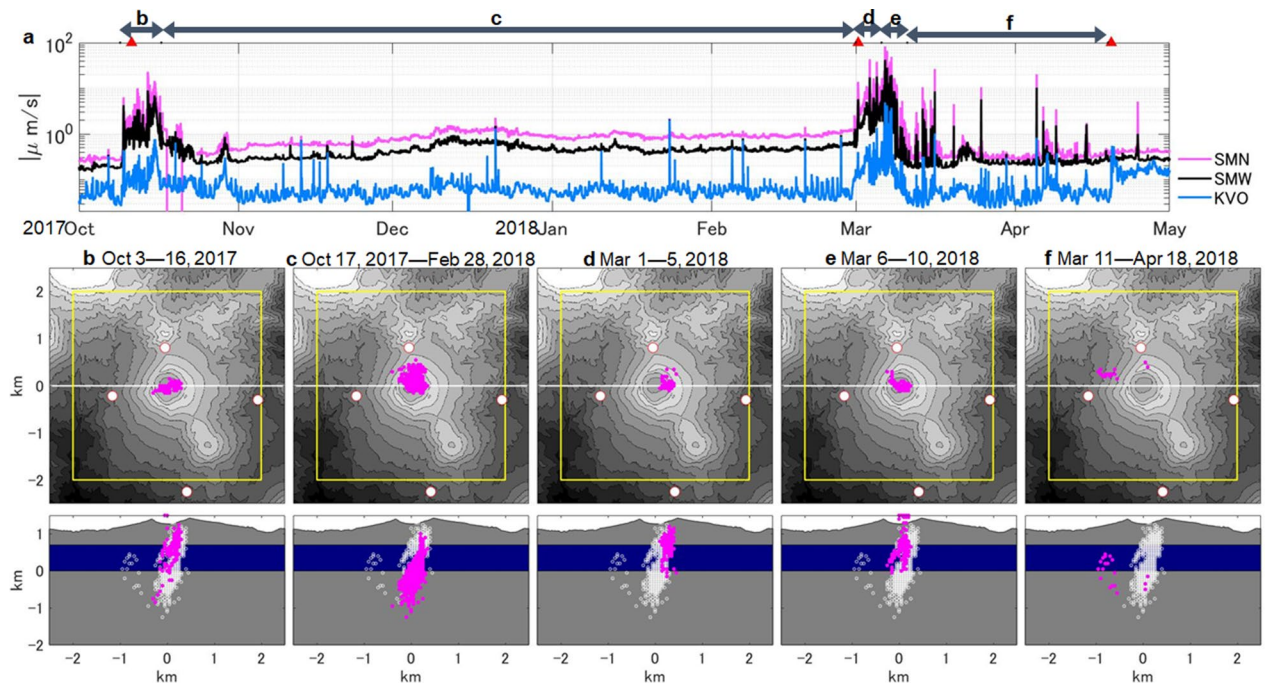

Fig. 5 a The variation of the continuous tremor amplitudes at 1–7 Hz at three stations as in the legend. The red triangles above the frame mark the onsets of the 2017 and 2018 eruptions of Shinmoe-dake. **b–f** The source locations of the continuous tremors in the periods indicated above the panel **a** are shown by magenta dots, and those in the whole period are by white dots. Some sources are located above the ground during the eruptions by errors (**b** and **e**). The red circles are the stations, and the yellow square represents the area in which the source was searched. The vertical section along the white line is shown in the bottom panel. The blue layer indicates the water-layer depth suggested by the resistivity structures (e.g., Kagiyama et al. 1996; Utada et al. 1994).

Data set and methods
Observation
All times in this paper are in Japan Standard Time (UTC + 9 h).

The seismic stations used in this study are shown in Fig. 1e. They were operated by the Earthquake Research Institute of the University of Tokyo (ERI), JMA, and NIED (see the legend). Most seismometers were broadband, but some were short-period instruments (Additional file 1: Table S1). Some stations were equipped with infrasound sensors (e.g., EBS and KVO: MB2005 of Dase, SMW:SI104 of Hakusan Co., and KITK: 7144/3348 of ACO Co.). Based on the calibration using common signals (Vulcanian explosions of Shinmoe-dake and

Ichihara *et al. Earth, Planets and Space* (2023) 75:144

Page 8 of 21

Sakurajima), we found that the amplitude and waveform of KITK were unreliable. However, the data were useful for signal detection using the cross-correlation analysis with other stations. All the seismic and infrasonic data were telemetered with a sample rate of 100 Hz.

Several monitoring cameras recorded Shinmoe-dake and Iwo-yama, operated by the JMA and the Kagoshima Prefecture (arrowheads in Fig. 1e). Occasional surveys were made on-site or from aircraft by JMA, the local governments, and the media with researchers. We collected their photos, the monitoring camera images reported by JMA (Fig. 2), and satellite images (Fig. 3).

Permanent continuous global navigation satellite system (GNSS) stations were operated by the GSI (the vertices of the black triangle in Fig. 1e). They were used to calculate the areal strain, which represented the year-scale inflation at the ~10-km-deep source (Fig. 4a) (e.g., Nakao et al. 2013; Yamada et al. 2019; Nishida et al. 2020).

Seismic data analyses

We analyzed the seismic and infrasonic data using methods that were already published. We made efforts in the visualization of the results to highlight the eruption sequences.

We mainly used the frequency range of 1–7 Hz, so we only converted the voltage to the mechanical unit (μ m/s) without correcting for the individual instrumental responses. We calculated the seismic power spectral density (PSD) using the three-component ground velocity data every 10 s. The signal power at the ith station, P_i (hereafter, the subscript denotes the station), was calculated by integrating the PSD in a target frequency range. Then, the observed amplitude, A_i^{obs}, was defined as a square-root of the averaged P_i in a time window. We used different averaging depending on the purpose, as described below.

Seismic background level (SBL)

Fig. 4b shows the SBL in 3.5–7 Hz (Ichihara et al. 2023). To calculate a daily SBL, we used a 6-h-long time window in nighttime (18:00–24:00 and 24:00–6:00) and took the 20th percentile (the lowest 20-% value in the window) as the average. To exclude the fluctuation due to weather conditions, we further took the 20th percentile of the daily SBLs in a 7-day time window (Ichihara et al. 2023). The results are shown after corrected for the site amplification that we evaluated in 3.5–7 Hz (see below).

Long-term amplitude change of the continuous tremor

Fig. 5a shows A_i^{obs} in 1–7 Hz, which was calculated as a square-root of a median of P_i in a 10-min-long time window sliding every 5 min. The results are shown without the site correction.

Source location of the continuous tremors

Fig. 5b–f shows the source locations of the continuous tremors. We followed the protocol of Ichihara and Matsumoto (2017) using the amplitude-based source location method (Battaglia and Aki 2003). Note that this method estimates only continuous tremor sources, excluding transient signals like isolated LF events and short tremors. The protocol used the frequency range of 3.5–7 Hz and calculated A_i^{obs} as the median of P_i every 5 min. We selected the time windows to search for the source location by examining the steadiness of the amplitude ratios for all pairs of the stations shown by the red circles in Fig. 1e. Time windows in which any of the stations had problems were excluded. Ichihara and Matsumoto (2017) used seven stations around Shinmoe-dake operated in 2011 and calibrated the site amplification factor, S_i, and the attenuation factor, B, referring to the continuous tremor source determined by a dense seismic array. In this study, we calibrated S_i and B in 3.5–7 Hz using the data from 9:00–12:00 on March 3, 2018, assuming the source was beneath the ash-emitting vent at the eastern edge of the crater (Fig. 2c). The reference source depth was determined as 700 m above the sea level to fit the amplitude distribution best by the model (Ichihara and Matsumoto 2017). The source location was estimated so that the observed amplitude ratio between station pairs, $R_{ij}^{obs} = A_i^{obs}/A_j^{obs}$, was the best fit by the model,

$$R_{ij}^{model} = \frac{S_i D_i^{-1} \exp(-BD_i)}{S_j D_j^{-1} \exp(-BD_j)}, \tag{1}$$

where D_i is the source–receiver distance. For each selected time window, we searched the location to minimize the fitting residual, *RES*, defined by

$$RES = \sqrt{\frac{2}{N(N-1)} \Sigma_{i=1}^{N-1} \Sigma_{j=i+1}^{N} \left(\frac{R_{ij}^{obs} - R_{ij}^{model}(D_i, D_j)}{R_{ij}^{model}(D_i, D_j)} \right)}. \tag{2}$$

We considered the results referring to the minimum *RES* values (RES_{min}). Figure 5b–f shows the sources determined with $RES_{min} < 0.22$. The source depths during the 2017 and 2018 eruptions are presented in Figs. 6d and 7d for $RES_{min} < 0.3$. The colors indicate the RES_{min} values of the individual points (see the caption), demonstrating that the sources were estimated consistently in this range of the fitting residual.

Tremor amplitude variation during the eruptions

Figures 6a and 7a show the amplitude variation at 1–7 Hz during the 2017 and 2018 eruptions. Here, we calculated the average of P_i in 2-min windows. To highlight the explosions as well as the continuous tremors, we took the

Ichihara *et al. Earth, Planets and Space* (2023) 75:144

Page 9 of 21

mean value of P_i, instead of the median or percentile. To reduce the influences of the outliers mainly due to missing data or electric noise, we excluded the maximum and minimum values of P_i in each window in calculating the mean. The results are shown without the site correction.

Infrasonic data analyses

The infrasound signals during the 2017–2018 eruptions were generally weak except for the Vulcanian explosions (Yamada et al. 2019). We searched for the signals using the cross-correlation between sensor pairs (Muramatsu et al. 2021) among EBS, SMW, KITK, and KRS (Fig. 1e). We calculated the cross-correlation coefficient, C_{ij}, in 1–7 Hz in 10-s time windows and averaged for 2 min. Figures 6c and 7c show C_{ij} between KITK and EBS as functions of the time of the window and the time delay of the KITK to EBS. The delay times of the correlation peaks in Figs. 6c and 7c vary within the range of − 2 s and 2 s. The change in apparent sound speed cannot explain the variations. They should represent the change of the source location within the crater area (Additional File 2).

Figures 6b and 7b show the amplitudes variation of infrasound data at EBS and KITK, calculated in the same way as Figs. 6a and 7a. When the two lines are coherent, and C_{ij} exhibits a clear correlation in the delay time range, we regard that the values represent the intensity of infrasound from Shinmoe-dake.

Eruption sequences of the 2017–2018 Shinmoe-dake and Iwo-yama volcanic activity

This section describes the eruption sequence of the 2017–2018 Shinmoe-dake eruption and the associated small eruptions that occurred on Iwo-yama in 2018.

Volcanic activity on Shinmoe-dake in 2017

The GNSS observations revealed deep inflation of Kirishima volcano from around July 2017 (JMA 2017a) (Fig. 4a). Also, the two seismic stations close to Shinmoe-dake crater (SMN and SMW in Fig. 1e) exhibited a gradual increase of the SBL (Ichihara et al. 2023) (Fig. 4b). The 2017 eruption started on October 11, 2017. The eruption was much smaller than the 2011 eruption and produced tephra less than 10^9 kg. The lava effusion was not observed (Table 1).

The following sequence of the event has been reported (all dates are in 2017):

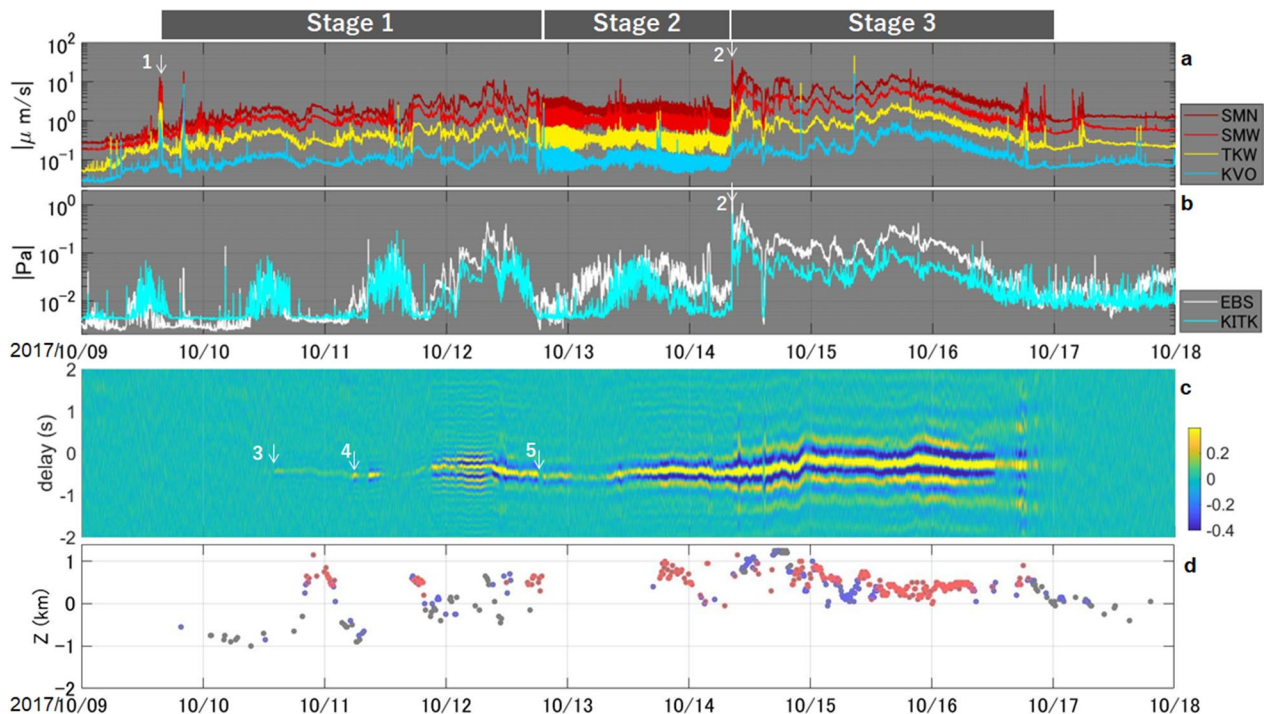- At approximately 15:10 on October 9 (arrow 1 in Fig. 6a), a tilt step and a swarm of low-frequency

Fig. 6 Seismic and infrasonic signals during the 2017 eruption. **a** Variation of the amplitudes of the seismometers in 1–7 Hz. **b** That of infrasound sensors in 1–7 Hz. **c** The cross-correlation coefficient as a function of the time delay of KITK to EBS. **d** The depth of the located continuous tremors. The red, blue, and gray colors indicate RES_{min} below 0.15, between 0.15 and 0.22, and between 0.22 and 0.3, respectively. Arrows with numbers indicate the features discussed in the text

Ichihara *et al. Earth, Planets and Space* (2023) 75:144

Page 10 of 21

earthquakes (LF) were recorded (Yamada et al. 2019). Then, volcanic tremors were recognized (JMA 2017a; Yamada et al. 2019).

- At 05:34 on October 11, a small eruption occurred at the eastern margin of the summit crater, and an ash plume rose 300 m above the crater (Fig. 2a) (JMA 2017a, b). The eruption continued until 16:00 on October 13, which deposited a thin ash layer over the eastern areas of the volcano (JMA 2017a).
- From 06:50 to 09:20 on October 12, the volcanic tremor amplitude became larger, and the plume reached higher than 1700 m above the crater.(JMA 2017b).
- From 19:30 on October 12 to 08:10 on October 14, the tremor amplitude cyclically increased and decreased, during which the plume was 100–300 m above the crater (JMA 2017b).
- At 08:23 on October 14 (arrow 2 in Fig. 6a), the eruption resumed with the ejection of a gray–white ash plume that rose 2300 m above the crater and spread ash-fall deposits over a wide area (JMA 2017a, b).
- On October 15, SO_2 was released at 11000 tons/day, which was comparable with the sub-Plinian phase of the 2011 eruption. It significantly decreased by the following day (JMA 2017a).
- At 00:30 on October 17, the monitoring camera image confirmed that the second ash emission had stopped (Yamada et al. 2019).

Based on our seismo-acoustic analyses and the above reports, we classify the 2017 eruption into three stages: Stage 1, from October 9 to around 18:00 on October 12; Stage 2, from then to 08:23 on October 14; Stage 3, from then to the end of October 16.

Stage 1 (ash emission: from october 9 to around 18:00 on october 12)

On the morning of October 9, the increase in the tremor amplitude was already evident (Fig. 6a). At 14:04 on October 10, the first infrasound signal was detected (arrow 3 in Fig. 6c), which may be associated with the increase of the white plume that JMA (2017b) reported. The tremor source was initially deep ($\sim$ 1 km below sea level, hereafter denoted as bsl), moved to very shallow depths, and stayed there from 20:30 on October 10 to 02:00 on 11 (Fig. 6d). The tremor source became deep again, and the reported eruption at 05:34 occurred with a clear infrasound signal (arrow 4 in Fig. 6c). The sensor-pair time delay (-0.5 s for KITK-to-EBS in Fig. 6c) was consistent with the observation that the vent was at the eastern margin of the crater (Fig. S2). From 20:40 on October 11 to about 10:00 on October 12, both seismic

and infrasonic tremor amplitudes were relatively large. This period included the plume height of 1700 m mentioned above. Infrasound decayed gradually to the evening and became unclear around 18:00 (arrow 5 in Fig. 6c), but the seismic tremor amplitude changed differently (Fig. 6a).

Stage 2 (cyclic tremor variation from 18:00 on october 12 to 08:23 on october 14)

In this stage, the tremor amplitude has a unique cyclic feature (Fig. 6a), as has been reported (JMA 2017b). The tremor cycles accompanied infrasound cycles, which are clear at low wind noise (Fig. 8a, b). The tremor sources were not determined in our current method targeting continuous tremors. The last cycle ended at 08:19 on October 14 before the explosion at 08:23.

Stage 3 (main phase from 08:23 on October 14 to october 17)

At 08:23 on October 14, when the eruption resumed, impulsive seismic and infrasonic powers were observed (arrows 2 in Fig. 6a, b). From then to 12:00 on October 16, the infrasound amplitude was relatively large. In this period, especially after October 15, both infrasound and seismic tremor amplitudes grew coherently (Fig. 6a, b). The feature was similar to the sub-Plinian phases in the 2011 eruption, suggesting that the eruption mechanism was steady (Ichihara 2016). The largest SO_2 emission rate occurred in this period. Both seismic and infrasonic tremor amplitudes decayed exponentially over October 16.

Volcanic activity on Shinmoe-dake in 2018

The deep inflation of the Kirishima volcano and the increase of the SBL had not stopped after the 2017 eruption (JMA 2018a; Ichihara et al. 2023) (Fig. 4). On March 1, 2018, approximately four months after the October 2017 eruption, a new activity was observed at Shinmoe-dake. Matsumoto and Geshi (2021) divided this activity into three stages. Referring to their classification, we defined the following three stages of volcanic activity: Stage 1 (ash emission: March 1–5); Stage 2 (lava effusion: March 6–8); Stage 3 (Vulcanian eruptions: March 9–June). Although Matsumoto and Geshi (2021) defined the start of Stage 3 on March 10, we set it on March 9 because the lava effusion had declined considerably by March 8, and the Vulcanian eruptions started on March 9 (described below in Stage 3). The features of the seismic and infrasonic activity also supported our definition (Fig. 7a, b). The 2018 activity followed a similar eruption sequence to the 2011 eruption, except for the lack of sub-Plinian eruptions.
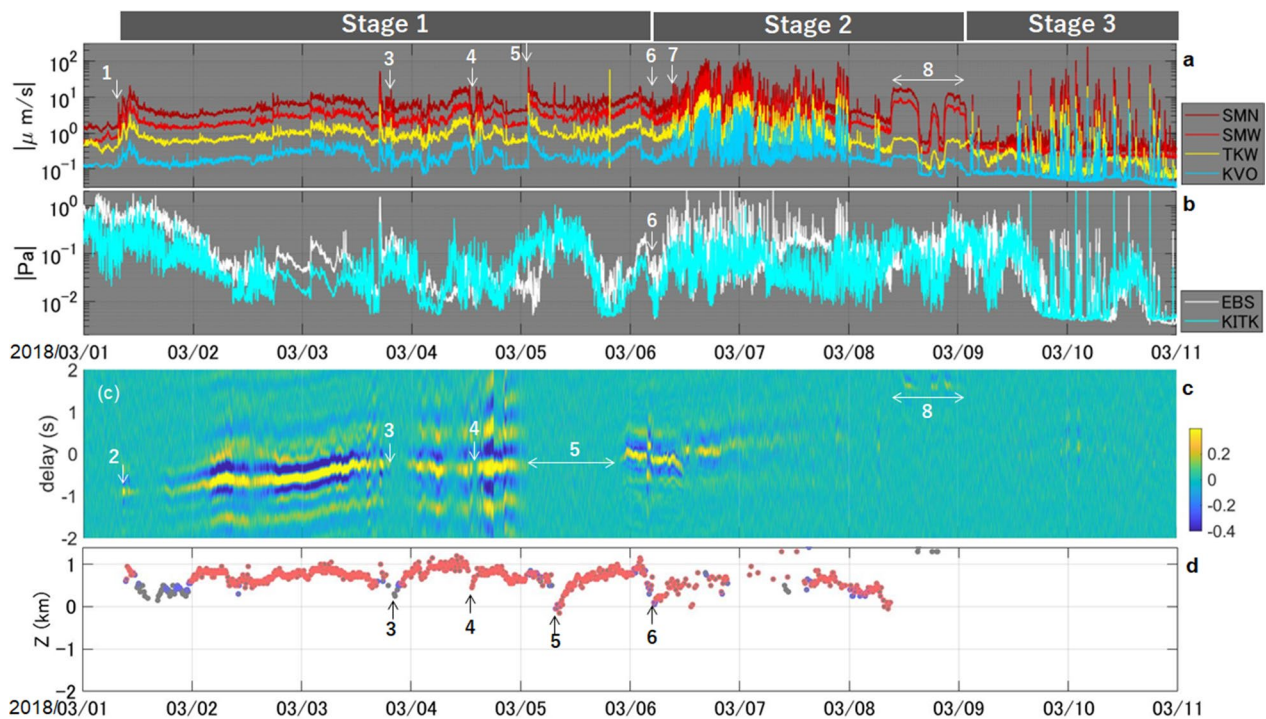
Ichihara *et al. Earth, Planets and Space* (2023) 75:144

Page 11 of 21

Fig. 7 Seismic and infrasonic signals during the 2018 eruption. Variation of the amplitudes of the seismometers in 1–7 Hz (**a**) and infrasound sensors in 1–7 Hz (**b**). **c** The cross-correlation coefficient as a function of the time delay of KITK to EBS. **d** The depth of the located continuous tremors. Arrows with numbers indicate the features discussed in the text

Stage 1 (ash emission: march 1–5)

The ash ejected during Stage 1 consisted mainly of non-juvenile materials, presumed to be composed of entrained preexisting rocks sourced from the 2011 lava when the vent opened (Matsumoto and Geshi 2021).

The following sequence of the event has been reported:

- At approximately 10:00 on March 1, the seismic amplitude increased due to increased tremors and LF events, but no particular change in the high-frequency (HF) events was found (Yamada et al. 2019).
- At approximately 11:00 on March 1, ash emissions started, depositing a small amount of ash on the eastern side of the Shinmoe-dake crater (JMA 2018a). It continued until March 9 (JMA 2018a) (Fig. 2c).
- Around 10:00 on March 2, aerial surveys revealed a plume rising from the vent at the eastern margin of the summit crater (JMA 2018a).
- On March 2, SO_2 emission was 5500 tons/day, and the level was likely maintained for this stage (JMA 2018a).
- On March 4, the monitoring camera confirmed that the ash emissions continued (Yamada et al. 2019).
- On March 5, the bad weather condition prevented the monitoring camera from capturing the activity, but JMA assumed that the eruption contin-

ued. From about 21:00, volcanic tremor amplitudes increased and the ash plume became more active (JMA 2018b).

Here, we additionally report the following:

- The continuous tremor had continued since the 2017 eruption (Fig. 5c). The source region was similar to the volcanic earthquake sources determined by JMA (JMA 2018a) and deeper than tremors during the eruptions (Fig. 5b,d,e).
- At 07:35 on March 1 (arrow 1 in Fig. 7a), the tremor amplitudes significantly increased at stations close to the Shinmoe-dake crater.
- At 08:30 on March 1 (arrow 2 in Fig. 7c), the first infrasonic signal was detected. The sensor-pair time delays (−0.9 s for KITK-to-EBS in Fig. 7c and −5.1 s for SMW-to-EBS) indicated that the source was at the eastern edge of the crater (Additional File 2: Fig. S2.1). Because the location is consistent with the vent location, the infrasound might represent the eruption onset or the vent opening. The signal was unclear between 12:00 and 16:00, probably due to the large wind noise. After the evening, the correlation became clearer and showed that the source shifted closer to the crater center.
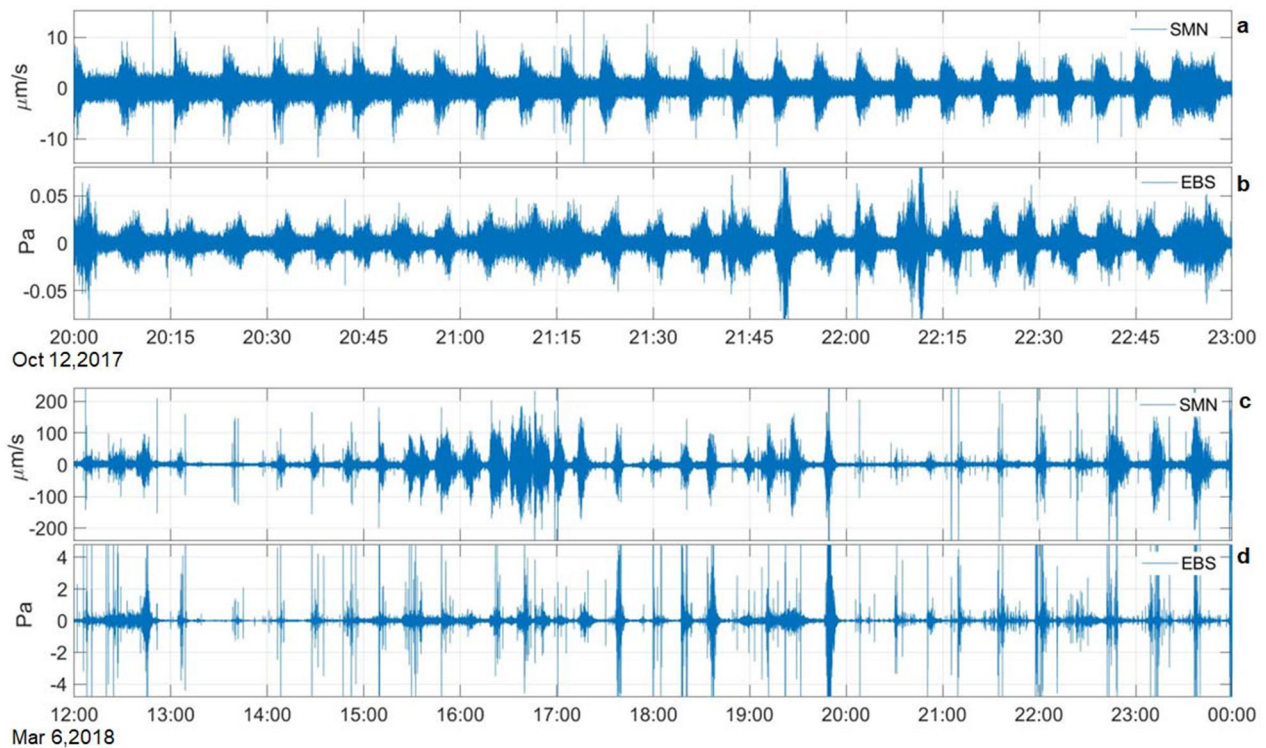
Ichihara *et al. Earth, Planets and Space* (2023) 75:144

Page 12 of 21

Fig. 8 **a**, **b** Cyclic events in Stage 2 of the 2017 eruption. **c**, **d** Cyclic events in Stage 2 of the 2018 eruption. The waveforms of the vertical component of the seismometer at SMN are detrended (**a** and **c**), and those of the infrasound sensor at EBS are filtered in 1–7 Hz (**b** and **d**)

- From ~01:40 to ~21:45 on March 5 (horizontal arrow 5 in Fig. 7c), infrasound signals were unclear. Although wind noise was strong on the day, we see only a subtle correlation even when the noise declined in the evening. Also, the disappearance of the infrasound signal coincided with the step-like increase of the seismic tremor amplitude around 01:40 (arrow 5 in Fig 7a). Therefore, we consider the volcanic activity was more significant below the surface than above the surface during the period. Interestingly, the tremor source depth changed from deep to shallow in this period (arrow 5 in Fig. 7d).
- Besides the above-mentioned period on March 5, infrasound signals became unclear in correlation with the deep-to-shallow change of the tremor source in 19:20–23:00 on March 3 (arrows 3 in Fig. 7a,c,d) and around 13:30–14:30 on March 4 (arrows 4 in Fig. 7a,c,d).

Stage 2 (lava effusion: march 6–8)

On March 6, lava began to effuse in the summit crater and spread across the preexisting 2011 lava flow (JMA 2018a) (Fig. 2d,e). The series of synthetic-aperture radar

SAR—satellite images from ALOS-2—Advanced Land Observing Satellite-2 showed that the lava effused from the northeastern part of the 2011 lava flow (about a few hundred meters to the northeast from the crater center) and spread in a circular manner from March 6 to 8, forming concentric pressure wrinkles on the surface (Figs. 1d and 3a–d). Based on the volume change estimated by the series of SAR satellite images, the lava effusion rate was estimated to be relatively constant at approximately 72 m³/s from March 6 to the morning of March 8 (NIED 2018a). From approximately 9:00 on March 6 to 12:00 on March 8, a tilt change showing deflation centered near Ebino-dake was observed (JMA 2018a; Yamada et al. 2019). This deflation period coincides with the lava effusion in the summit crater, which suggests that in the 2018 eruption, as in the 2011 eruption, magma moved from a magma reservoir below Ebino-dake at a depth of 6–10 km (Kobayashi et al. 2011; Nakao et al. 2013; Kozono et al. 2013, 2023) to an area below Shinmoe-dake where it effused (JMA 2018a; Yamada et al. 2019). The eruption in Stage 2 also included many small explosive events (JMA 2018a; Matsumoto and Geshi 2021). The ash ejected during Stage 2 was dominated by juvenile materials, which included bubble-rich magma fragments that may have caused the continuous ash emission

Ichihara *et al. Earth, Planets and Space* (2023) 75:144

Page 13 of 21

and bubble-poor magma fragments corresponding to the effusing lava (Matsumoto and Geshi 2021).

The detailed timeline has not been resolved, but the following have been reported:

- Between 03:00 and 06:00 on March 6, the lava effusion is supposed to start, based on the extrapolation of the satellite-driven lava accumulation rate (NIED 2018a).
- On March 6, vigorous plume emissions were observed from the lava flow center (Figs. 2d,e and 3c).
- On March 7, SO₂ emissions were 34000 tons/day, which was the highest recorded level in the 2018 activity (JMA 2018a).
- On March 6 and 7, cyclic amplitude changes were observed in seismic data due to increased LF events or quasi-monochromatic tremors around 1 Hz (Yamada et al. 2019). The cyclic events accompanied the inflation–deflation tilt cycles, which were evident only at the closest tilt station, KITK (Fig. 1e), and intermittent small explosive eruptions (plume height <3000 m) with infrasound (Yamada et al. 2019). A total of 34 small explosive eruptions were reported (JMA 2018a).
- On March 8, the lava discharge rate decreased abruptly and might have stopped on the day (NIED 2018a). The seismic activity was also temporarily reduced (Yamada et al. 2019).
- At 00:12 on March 9, ALOS-2 images suggest that the lava flow had grown to ca. 600 m in diameter (Fig. 3e) (GSI 2018a).

Here, we report additional information:

- Around 05:00 on March 6 (arrows 6 in Fig. 7a, b), the seismic and infrasonic amplitude variation started to be coherent. Also, the tremor source changed from the relatively deep location around the sea level (0 km) to the shallower (arrow 6 in Fig. 7d).
- Around 9:30 on March 6 (arrows 7 in Fig. 7a), the characteristic tremor cycles (Yamada et al. 2019) became apparent. They became less regular around 2:30 on March 7 and stopped at the end of March 7. All the tremor cycles accompanied infrasound, like October 12–14 (Fig. 8).
- From 09:18 to around 15:20 on March 8 (horizontal arrows 8 in Fig. 7a,c), the tremor amplitude became larger with infrasound signals. The cross-correlation time delays were significantly different from the previous signals (around 1.8 s for KITK-to-EBS and from −0.14 to −5.44 s for SMW-to-EBS in Additional File 3), indicating that the sources were at the western margin of the crater. The seismic amplitudes at the

closest two stations (SMN and SMW) are significantly larger than the other stations (Fig. 7a), indicating that the source was very close to these stations. On that day, the pancake lava in the crater was increasing its surface area toward the west. We suppose that the degassing vents on the crater floor were covered by the lava one after another. Then, the gas found a way to go out at the western edge of the lava with the seismic and infrasonic signals.

Stage 3 (intermittent vulcanian eruptions: march 9–june)

The lava effusion had stopped before March 9 (NIED 2018a), but the diameter of the accumulated lava in the crater increased by flattening due to the gravity (GSI 2018a; NIED 2018a). The diameter was about 600 m at 00:12 and 700 m at 12:05 on March 9 (Figs. 1d, 2f, and 3e). Later on March 10, the lava diameter became progressively larger, extending mainly to the west. It reached a final diameter of ∼730 m by mid-March (Fig. 3f–i) (GSI 2018a). Aerial SAR data collected on March 20, 2018, estimated the volume of the effused lava to be 1.6×10^7 m³, which is approximately the same as the amount of lava that effused at the summit in 2011, which was 1.5×10^7 m³ (Nakada et al. 2013b; Ozawa and Kozono 2013) (see Table 1 in weight). Assuming that the lava flow had a diameter of 730 m, the average thickness of this lava flow is estimated to be ca. 38 m. On approximately March 9, the northwestern tip of the lava flow began to flow down the slope from the lowest point of the crater rim for a distance of roughly 150 m down the slope until the movement ceased in mid-April (JMA 2018a) (Figs. 2h, 3e–i: the lava flow is indicated by arrows).

Stage 3 is characterized by Vulcanian explosions. These eruptions were larger in scale than the explosive eruptions in Stage 2, i.e., they either accompanied plumes rising higher than 3000 m, projectiles were ejected distances of more than 1000 m, or there were small-scale pyroclastic flows (JMA 2018a). These Vulcanian eruptions occurred around the center of the circular lava flow as in Stage 2 (Fig. 2g,i), and the ash ejected in Stage 3 was composed mainly of juvenile materials (Matsumoto and Geshi 2021). These materials are considered to be derived from the stagnant magma filling the summit crater (Matsumoto and Geshi 2021).

Because the signals are clearer in seismic, infrasonic, and tilt data (JMA 2018a; Yamada et al. 2019), the timelines in Stage 3 have been better constrained:

- At 15:58 of March 9, the first Vulcanian eruption in the 2018 eruption occurred (JMA 2018a; Yamada et al. 2019). (Fig. 2g).

Ichihara *et al. Earth, Planets and Space* (2023) 75:144

Page 14 of 21

- From March 9 to mid-March, the frequency of eruptions decreased to 2–3 times per day, on average, becoming increasingly sporadic after late March (JMA 2018a).
- On March 25 and April 5, small pyroclastic flows occurred with large eruptions (JMA 2018a).
- On March 9, the rate of SO_2 emissions was approximately 1000 tons/day, which was markedly lower than that in Stage 2 (JMA 2018a). Throughout Stage 3, the rate of SO_2 emissions had decreased gradually, reaching <100 tons/day after June (JMA 2018a).

Besides, we demonstrated the following:

- Aerial observations by one of the authors (TaKa) on March 13 showed that the eruption site formed a shallow lenticular depression with some pits near the center from which volcanic gas appeared to be emitted (Fig. 2k: indicated by yellow arrows). There was no clear topographic signature for the explosion crater, probably because the topography of the explosion site was erased by the flow of unconsolidated lava existing below as the surface solidification layer was thin at this stage.
- The eruption on April 5, on the other hand, formed a distinct concave topography as an explosion crater (Fig. 2l). This may be because the explosion was large, and surface solidification had progressed since the cessation of lava effusion, making it difficult for the lava to become deformed.
- The continuous tremor amplitude was low in Stage 3. Although it was difficult to determine the sources, their distribution was significantly different from those from the 2017 to the main phase of the 2018 eruption and shifted to the west, except for the three points in Fig. 5f at the north edge of the crater, which were determined when Vulcanian eruptions were active.
- SBLs at stations near Shinmoe-dake's crater (SMN and SMW) (Fig. 4b) decreased to similar levels as those after the 2017 eruption (the red dashed line) but remained significantly above the quiet level (the white dashed line) during Stage 3 but dropped suddenly at the end of May. After then, two eruptions occurred on June 22 and 27 (JMA 2018a).
- SBL at KVO close to Iwo-yama changed differently. It gradually increased from the beginning of April 2018 to the rapid increase at the Iwo-yama eruption. It dropped on May 18 and gradually decayed, while SBLs at stations closer to Shinmoe-dake abruptly terminated on May 31 (Fig. 4).

Volcanic activity on Iwo-yama in 2017 and 2018

Around Iwo-yama (Fig. 1c), an increase in hydrothermal activity, such as enlargement of high-temperature areas, was observed around December 2015 (Tajima et al. 2020). From February 2017, Iwo-yama's surface activity gradually increased (JMA 2017a), including the mud-pot appearance in March, the gradual tilt from April 25 to August 2017 (JMA 2017a), a tilt step and seismic swarms at shallow depths beneath Iwo-yama on September 5, and a steam blowout at Iwo-yama-south crater on April 26, 2017, from which ash fell in the surrounding areas (Tajima et al. 2020). The activity temporally declined after September 5 (JMA 2017a). Ohba et al. (2021), who investigated fumarolic gas at Iwo-yama, revealed an increase in magmatic vapor flux in May 2017 and late March 2018 while suppression of the flux from September 2017 to January 2018 (no data between January and March 2018). Results of the precise leveling reported some local deformation around Iwo-yama from late 2017 (Kyushu University 2018), but the corresponding deformation was unclear in GNSS baselines or SAR interferometry (JMA 2018c). The extension of the baselines of < 1 km around Iwo-yama became apparent from March 2018 until the April 19 eruption (JMA 2018a, c; GSI 2018b; NIED 2018b).

Small phreatic eruptions started at Iwo-yama-south crater at 15:39 on April 19, 2018 (Fig. 2n–p), shortly after the onset of the apparent volcanic tremors (Muramatsu et al. 2022) (Fig. 5a). Subsequently, multiple vents in the Iwo-yama south crater opened or activated (Muramatsu et al. 2021). This eruption generated a plume that rose to a height of 500 m, ash-fall deposited in the surrounding areas, projectiles spattered up to 100 m from the vent, and gushed large volumes of hydrothermal water (JMA 2018a). It was also reported that new fumarolic activity appeared in the Iwo-yama-west crater area around 16:30 on April 20 (JMA 2018a). Muramatsu et al. (2021) found corresponding infrasound signals that indicated multiple vent openings in the area. They also suggested that eruptive activity started in the area at 21:05. In addition, on April 26, small hydrothermal eruptions occurred on the Iwo-yama-west crater, generating ash-bearing plumes (JMA 2018a). SAR observations showed localized uplift around the Iwo-yama-south and Iwo-yama-west craters associated with the activity on April 19 and 26 (GSI 2018c).

Discussion

Figure 9 summarizes the event sequences that we presented above, and Table 1 compares the amounts of the eruption products in the past eruptions at Shinmoe-dake.

Ichihara *et al. Earth, Planets and Space* (2023) 75:144

Page 15 of 21

Here, we discuss the unique features of the 2017–2018 events in Kirishima.

The missing sub-Plinian phase

The 2018 eruption was the first confirmed eruption of Shinmoe-dake that was dominated by effusive activity lack in sub-Plinian phases. Saito et al. (2023) made petrological studies to investigate the difference between the 2011 and 2018 eruptions. They concluded that the 2018 magma was a remnant of the 2011 magma and had lower volatile content due to degassing in the magma reservoir. They explained the lack of the sub-Plinian phase in the 2018 eruption due to the lower volatile content. However, the bubble volume fractions in both magmas, which they estimated assuming a closed system, were large enough to infer fragmentation at shallow depth. This indicates that shallow degassing was necessary to prevent an explosive eruption, even in the 2018 eruption.

We regard the 2017 and 2018 eruptions of Shinmoe-dake as a sequential events because the year-scale inflation of the deep source and the SBL growth (Fig. 4) continued after the 2017 event toward the 2018 event. A significant amount of SO_2 comparable with the sub-Plinian phases of the 2011 eruption was emitted in the main phase (Stage 3) of the 2017 eruption, though the amount of tephra was limited. It indicates that the amount of magma and volatile involved in the eruption was comparable with the sub-Plinian eruptions, but the degassing was more efficient.

We consider the characteristic cyclic oscillations in Stage 2 of the 2017 activity (Fig. 8a) to be associated with degassing. The regularly repeating wave excitation suggests some non-linear feedback mechanism, like fluid flow through a flow-controlled or pressure-controlled valve (Lees and Bolton 1998; Lesage et al. 2006; Lyons et al. 2013) and a collapsible tube (Rust et al. 2008; Takeo 2020). Cyclic excitation of small low-frequency or hybrid earthquakes called 'drumbeat' earthquakes (Iverson et al. 2006; Moran et al. 2008; Bell et al. 2017) or 'swarm tremor' (Buurman et al. 2013) have been observed at many volcanoes associated with ascent and effusion of viscous magma (e.g., Iverson et al. 2006; Moran et al. 2008; Buurman et al. 2013) or sometimes without apparent lava effusion (Bell et al. 2017). Compiling 36 pre-eruptive seismicity patterns from 26 volcanoes, White and McCausland (2019) associated such repetitive events with the final ascent of magma at shallow depths. They also noted that repetitive events might only occur for minutes before explosive eruptions but may last for hours to days to months before passive dome extrusion. Such oscillations were considered to be generated with gas release and magma movement (Bell et al. 2017; Pallister
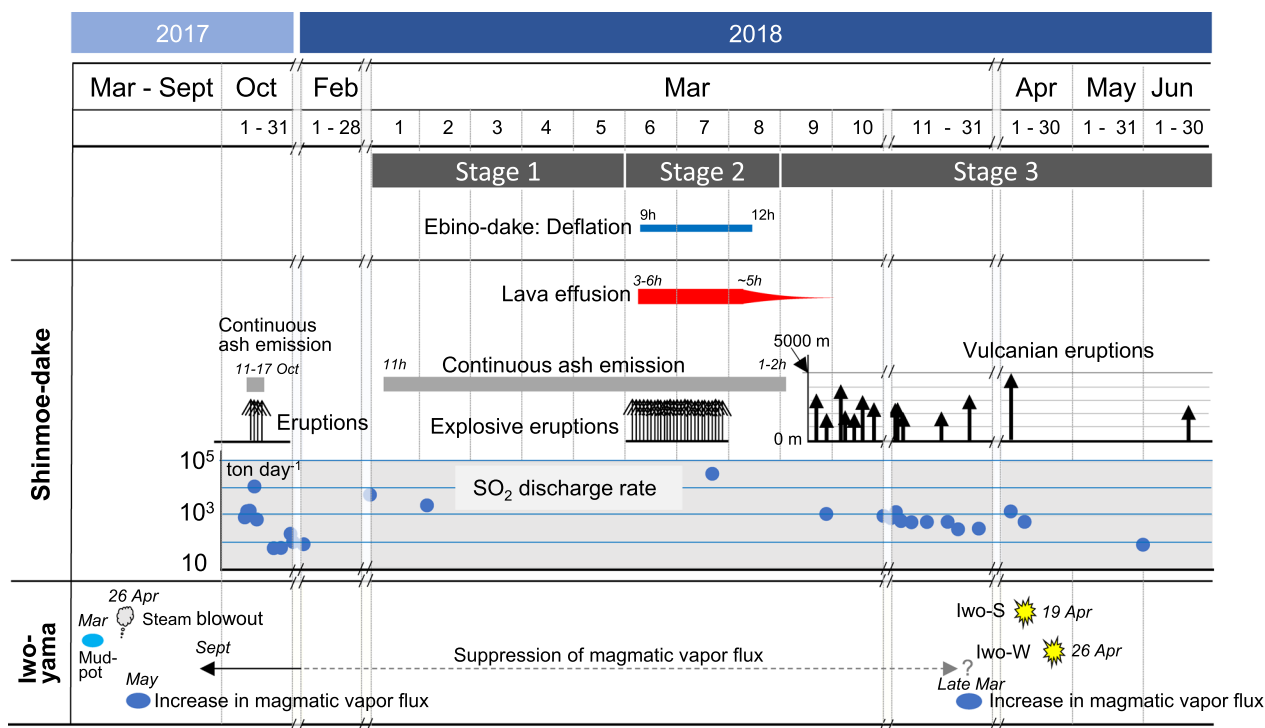

Fig. 9 Summary of the 2017–2018 volcanic activities on Shinmoe-dake and Iwo-yama

Ichihara *et al. Earth, Planets and Space* (2023) 75:144

Page 16 of 21

et al. 2013) or stick–slip motion of lava dome (Iverson et al. 2006). The repetitive occurrence of longer-duration tremors is called a 'banded tremor'. They are not necessarily related to eruptions and can be generated by a hydrothermal two-phase system, probably due to magmatic heat input (Fujita 2008; Cannata et al. 2010).

The cyclic tremor during the 2017 eruption of Shinmoe-dake accompanied weak infrasound (Fig. 8b). However, the gas separated from magma might not have been completely released to the atmosphere in each cycle. The gas accumulated at the shallow depth and erupted during Stage 3, leaving degassed magma behind.

After the 2017 eruption, the magma input to the shallow depth might have become active, as represented by the continuous tremor below the groundwater level (Fig. 5c). Then, the 2018 eruption occurred, erupting the degassed magma from the 2017 eruption together with new magma. The degassing was also efficient, represented by the cyclic tremor on March 6 and 7 in Stage 2 of the 2018 eruption (Fig. 8c). The duration and interval of the cyclic tremors are much longer ($\sim$ 30 min) than those in 2017. This time, the separated gas was released as small explosions generating strong infrasound (Fig. 8d) with ash, and the remaining magma erupted as lava simultaneously.

In the above story, the cyclic oscillation might make evidence of degassing but not the cause. We infer the difference between the 2017–2018 eruptions and the 2011 eruption is the interval from the previous magmatic eruption. The 2011 eruption occurred 300 years after the previous major magmatic eruption, while the 2017–2018 eruption occurred shortly after the 2011 eruption. The magma pathway might have been warmer, which kept the ascending magma warmer and prevented fragmentation, even if the magma was similar to that of 2011.

It has been considered that Shinmoe-dake is an example of less-frequent eruption (Nakada et al. 2013a), based on the geological and historical eruption records. However, finding geological evidence of eruptions like the 2018 event could be difficult. An effusive-dominated eruption was documented for the first time at Shinmoe-dake in 2018 by modern methods, including geophysical data, areal photos, and satellite observations. Because Shinmoe-dake and most of the other cones in the Kirishima volcanic group have large craters, they can tap a significant amount of lava, preventing it from overflowing onto the flanks. Such lava may not necessarily leave clear evidence on the edifice and might have been covered or lost by the following eruptions. Therefore, eruptions dominated by effusive styles could have been more frequent than have been thought.

Relationship between Shinmoe-dake and Iwo-yama activity

Both Shinmoe-dake and Iwo-yama had eruptions in 2018. Here, we discuss the link between the two cones.

Ohba et al. (2021) proposed the following scenario. Early in 2017, magma was supplied from the deep reservoir (the inflation source at a depth of around 10 km) to a shallow silicic magma reservoir beneath Iwo-yama, from which magmatic gas was released to Iwo-yama. Sometime between May and September 2017, the formation of the sealing zone above the silicic reservoir prevented gas emission and triggered the gas transport to Shinmoe-dake, leading to the eruptions. In late March 2018, after the main phase of the 2018 eruption of Shinmoe-dake, the breakage of the sealing zone restarted the large magmatic gas flux at Iwo-yama and triggered its 2018 eruption. On the other hand, Tsukamoto et al. (2022) considered that the formation and breakage of sealing occurred at a clay layer about few hundred meters beneath Iwo-yama, which controlled the shallow inflation in 2017 and the phreatic eruption in 2018.

The recent activities of Shinmoe-dake and Iwo-yama seem to be alternating. The hydrothermal activity of Iwo-yama declined before 2008 (Tajima et al. 2020), and Shinmoe-dake became active in 2008 and had the 2011 eruption (Nakada et al. 2013b). Then, Iwo-yama resumed being active in late 2015 (Tajima et al. 2020) and increased its activity in 2017 (Fig. 9). Although the year-scale growths of the deep inflation and the shallow seismic noise (SBL) presented in Fig. 4 have been considered to represent the eruption preparation of Shinmoe-dake, according to the case of the 2011 eruption (e.g., Nakao et al. 2013; Nakada et al. 2013b; Yamada et al. 2019; Ichihara et al. 2023), the surface activity appeared at Iwo-yama instead of Shinmoe-dake, which is contrasting to the pre-2011 eruption case.

Combining models proposed by Ohba et al. (2021) and Tsukamoto et al. (2022) with the data set that this study collected, we propose a scenario illustrated in Fig. 10. We employ models of the seismic velocity structure beneath the Kirishima Volcanic Group (Nagaoka 2020; Nishida et al. 2020), the resistivity structure beneath Kirishima (Utada et al. 1994; Kagiyama et al. 1996, 1997; Aizawa et al. 2014; Tsukamoto et al. 2022), the deep inflation source for the geodetic data (Nakao et al. 2013), and deep low-frequency earthquake sources (Kurihara et al. 2019; Kurihara and Kato 2022).

The pressure increase in the basaltic magma reservoir (sill complex) brought magma beneath Shinmoe-dake at a shallow depth, using a similar pathway as the 2011 eruption magma pathway. The magmatic gas was released
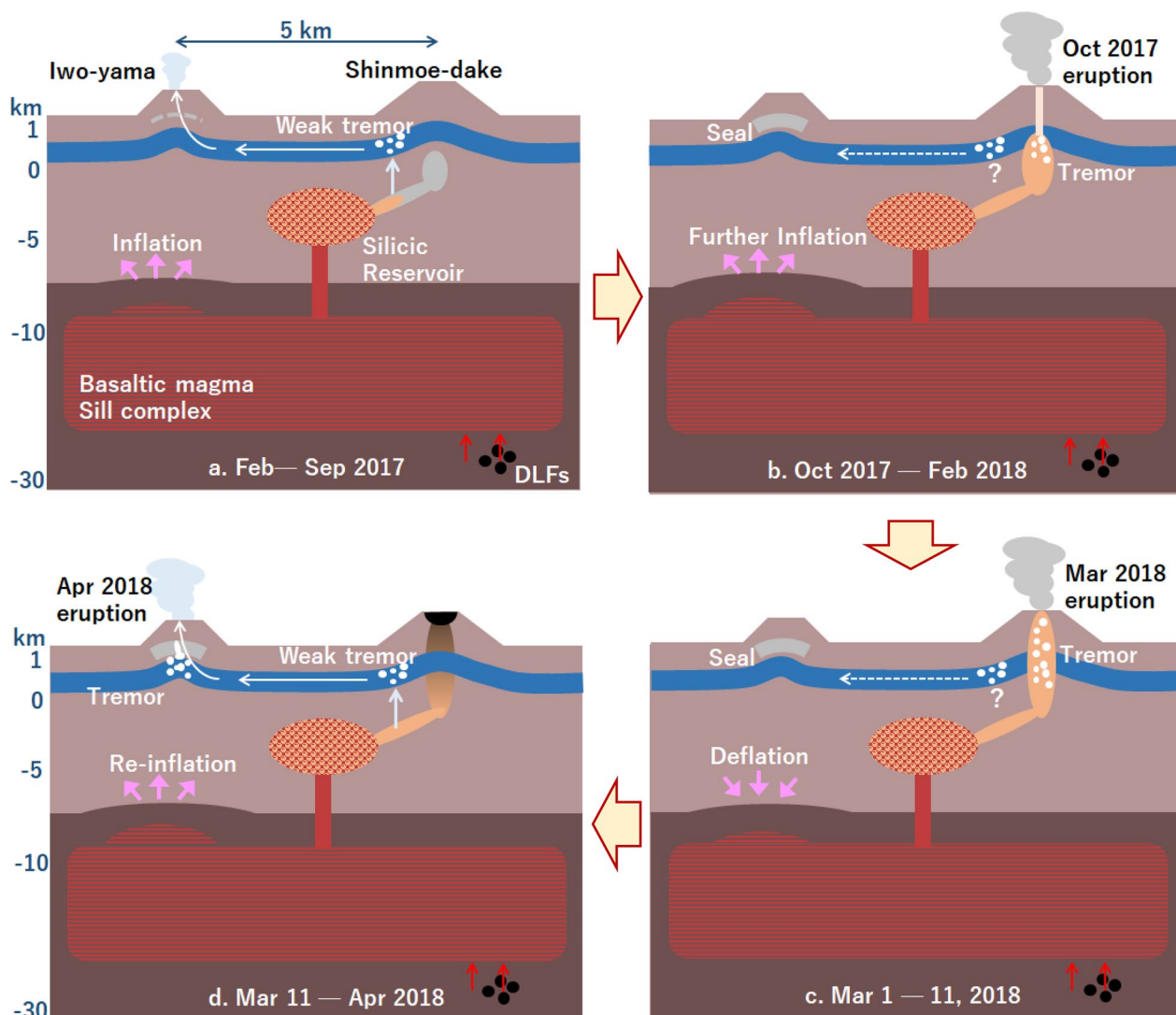
Ichihara *et al. Earth, Planets and Space* (2023) 75:144

Page 17 of 21

Fig. 10 A model for the sequences of the 2017–2018 eruptions of Shinmoe-dake and the 2018 eruption of Iwo-yama. The underground structures follow models based on seismic interferometry (Nagaoka 2020; Nishida et al. 2020) and the magnetotelluric analyses which presented a continuous shallow low-resistivity layer between Shinmoe-dake and Iwoyama (Aizawa et al. 2014) and fluid pathways beneath Iwo-yama (Tsukamoto et al. 2022). We also referred to Kurihara and Kato (2022) for the DLF earthquake sources and their implications and Ohba et al. (2021) for volatile transport. **a** Pre-eruption period. **b** From the 2017 eruption to before the 2018 eruption of Shinmoe-dake. **c** During the 2018 eruption. **d** From the 2018 eruption of Shinmoe-dake to the 2018 eruption of Iwo-yama

from there, and groundwater was heated, increasing seismic noise (weak tremor) observed as SBL (Fig. 10a). The noise source was certainly closer to Shinmoe-dake than Iwo-yama because they were evident at stations close to Shinmoe-dake crater (SMN and SMW), but not at the station close to Iwo-yama (KVO) (Figs. 1e, 4b). On the other hand, surface gas flux was evident at Iwo-yama instead of Shinmoe-dake (Fig. 9). Before October 2017, the gas release from Iwo-yama was prevented by the formation of sealing (Fig. 10b). Then, the 2017 eruption of Shinmoe-dake occurred. After the eruption, the continuous tremor below the sea level became active in

early November, which evidences the magmatic activity beneath Shinmoe-dake. It is not clear whether the gas transport to Iwo-yama continued during this period. Then, the 2018 eruption of Shinmoe-dake occurred, and the deep sill complex deflated (Fig. 10c). After March 11, 2018, when the eruptions and magmatic tremor at Shinmoe-dake declined, the hydrothermal tremor at the shallow depth in the west flank of Shinmoe-dake became apparent (Fig. 5f). The volatile transport to Iwo-yama became active because the vents at Shinmoe-dake were plugged by the lava. Pressure at a shallow depth beneath

Ichihara *et al. Earth, Planets and Space* (2023) 75:144

Page 18 of 21

Iwo-yama increased to trigger its eruption in April (Fig. 10d).

The relationship between Shinmoe-dake and Iwo-yama eruptions in Fig. 10 follows the model of Ohba et al. (2021), but we assume the shallow volatile transport instead of the fluid pathway from the depth of ~5 km. The reason is that we found no sign of fluid movement from a deep source to Iwo-yama, at least before the 2018 eruption of Shinmoe-dake. Besides the above-mentioned lack of SBL sources around Iwo-yama, volcanic earthquakes at Iwo-yama were also limited at shallow depths (JMA 2018a). Recently, Yukutake et al. (2023) re-examined volcanic earthquakes in Kirishima from 2008 to 2019. They showed that the earthquakes at Iwo-yama started increasing in 2014, and the source depth range gradually shifted upward from ~0.5 km bsl to 0 km from 2015 to March 2018. However, the seismic event rate did not accelerate, contrasting with the SBL near Shinmoe-dake. From the 2018 eruption of Shinmoe-dake to the 2018 eruption of Iwo-yama, the volcanic earthquakes at Iwo-yama increased and distributed down to 1.0 km bsl. Vertical fluid transport, if any, may have occurred in this period. The SBL at the station closest to Iwo-yama (KVO) started increasing in April, though the SBLs near Shinmoe-dake remained higher than at KVO (Fig. 4b).

Summary

This study reported the detailed sequence of the recent eruptions at Shinmoe-dake and Iwo-yama of the Kirishima Volcanic Group. By combining documents, photos (Fig. 2), and satellite images (Fig. 3), the surface activities are summarized in Fig. 9. We also presented new results of seismo-acoustic analyses, including the growth of seismic background level compared with deep inflation (Fig. 4), continuous tremor source locations beneath Shinmoe-dake (Fig. 5), and seismo-acoustic signals during the 2017 and 2018 eruptions of Shinmoe-dake (Figs. 6 and 7), which helped us identify three stages for each of the two eruptions. The second stage of both eruptions exhibited regularly repeated tremors, which we interpreted as a sign of gas separation from magma, referring to global examples. We consider that the effective degassing explains the lack of sub-Plinian phase in the 2017–2018 eruptions, contrasting with the 2011 eruption. The timelines (Fig. 9) exhibited that the surface activities of Shinmoe-dake and Iwo-yama were alternating in 2017–2018. On the other hand, the continuous tremor and long-lasting noise identified as seismic background level were dominant around Shinmoe-dake, while seismic activity around Iwo-yama became apparent only after the 2018 eruption of Shinmoe-dake. Combining these findings with the previous studies, we propose a sequential model for the eruptions (Fig. 10).

The eruptions were the first effusion-dominated eruption at Shinmoe-dake and the first successive eruptions of two cones that have ever been reported at Kirishima. These eruptions allow us to understand better the magma supply systems and behaviors of the Kirishima Volcanic Group. Although our model is still preliminary, it explains the current data set the best and poses questions to future studies.

Abbreviations

ERI   The Earthquake Research Institute of the University of Tokyo
JMA   The Japan Meteorological Agency
NIED   The National Research Institute for Earth Science and Disaster Resilience
GSI   The Geospatial Information Authority of Japan
GNSS Continuous global navigation satellite system
SBL   Seismic background level
SAR   Synthetic-aperture radar

Supplementary Information

The online version contains supplementary material available at https://doi.org/10.1186/s40623-023-01883-8.

Additional file 1: Table S1. Station information.

Additional file 2. Expected infrasound time delays between sensor pairs.

Additional file 3. Additional information of the seismo-acoustic signals in Stages 2 and 3 of the 2018660 eruption at Shinmoe-dake.

Author contributions

MI and TaKa drafted the manuscript. MI made seismo-acoustic data analyses and their interpretation. TaKa collected the aerial and satellite images and reported information. TsKo checked the information from JMA, FM confirmed the geological information. SN provided observational photos, and TO and AW mainly worked on the seismo-acoustic observation. All the authors discussed the manuscript.

Availability of data and materials

The datasets used and/or analyzed during the current study are available from the corresponding author on reasonable request.

Declarations

Competing interests

There is no competing interests.

Ichihara *et al. Earth, Planets and Space* (2023) 75:144

Page 19 of 21

Author details
[1]The Earthquake Research Institute, The University of Tokyo, Tokyo 113-0032, Japan. [2]Japan Meteorological Agency, Tokyo, Japan. [3]The National Research Institute for Earth Science and Disaster Resilience, Tsukuba, Japan.

References
Aizawa K, Koyama T, Hase H, Uyeshima M, Kanda W, Utsugi M, Yoshimura R et al (2014) Three-dimensional resistivity structure and magma plumbing system of the Kirishima Volcanoes as inferred from broadband magneto-telluric data. J Geophys Res Solid Earth 119:198–215. https://doi.org/10.1002/2013JB010682

Battaglia J, Aki K (2003) Location of seismic events and eruptive fissures on the Piton de la Fournaise volcano using seismic amplitudes. J Geophys Res 108:2364. https://doi.org/10.1029/2002JB002193

Bell AF, Hergandez S, Gaunt HE, Mothes P, Ruiz M, Sierra D, Aguaiza S (2017) The rise and fall of periodic 'drumbeat' seismicity at Tungurahua volcano, Ecuador. Earth Planet Sci Lett 475:58–70. https://doi.org/10.1016/j.epsl.2017.07.030

Buurman H, West ME, Thompson G (2013) The seismicity of the 2009 Redoubt eruption. J Volcanol Geotherm Res 259:16–30

Cannata A, Di Grazia G, Montalto P, Ferrari F, Nunnari G, Patané D, Privitera E (2010) New insights into banded tremor from the 2008–2009 Mount Etna eruption. J Geophys Res-Solid Earth 115:B007120. https://doi.org/10.1029/2009JB007120

Fujita E (2008) Banded tremor at Miyakejima volcano, Japan: Implication for two-phase flow instability. J Geophys Res-Solid Earth 113:B04207. https://doi.org/10.1029/2006JB004829

Geshi N, Takarada S, Tsutsui M, Mori T, Kobayashi T (2010) Products of the August 22, 2008 eruption of Shinmoedake Volcano, Kirishima Volcanic Group, Japan. Bull Volcanol Soc Jpn 55:53–64. https://doi.org/10.18940/kazan.55.1_53

GSI (2018a) Analysis of topographic change of the Kirishima volcano (Shinmoe-dake) using airborne SAR data. https://www.gsi.go.jp/common/000199110.pdf. Accessed 16 July 2022

GSI (2018b) Response to the 2018 eruption of Mt. Kirishima (Ebino area (Iwoyama) and vicinity) https://www.gsi.go.jp/BOUSAI/h30kirishima_ebino.html. Accessed 16 July 2022

GSI (2018c) Report for Coordinating Committee for Prediction of Volcanic Eruptions 140:116–119. https://www.https://www.data.jma.go.jp/svd/vois/data/tokyo/STOCK/kaisetsu/CCPVE/shiryo/140/140_01-2.pdf Accessed 22 July 2023

Ichihara M (2016) Seismic and infrasonic eruption tremors and their relation to magma discharge rate: A case study for sub-Plinian events in the 2011 eruption of Shinmoe-dake, Japan. J Geophys Res-Solid Earth 121:7101–7118. https://doi.org/10.1002/2016JB013246

Ichihara M, Matsumoto S (2017) Relative source locations of continuous tremor before and after the subplinian events at Shinmoe-dake, in 2011. Geophs Res Lett 44:10871–10877. https://doi.org/10.1002/2017GL075293

Ichihara M, Ohminato T, Konstantinou K et al. (2023) Seismic background level growth can reveal slowly developing long-term eruption precursors. (submitted to Sci Rep) https://doi.org/10.21203/rs.3.rs-2501205/v1

Imakiire T, Oowaki A (2011) Source Model of Kirishima Volcano Based on GPS Integrated Analysis in Volcanic Region. Report of Geospatial Information Authority of Japan, 121: 183-188. https://www.gsi.go.jp/common/000062557.pdf. Accessed 16 July 2022

Imura R (1992) Minor phreatic activity of Shinmoedake, Kirishima volcanoes, in 1991–1992. Bull Volcanol Soc Jpn 37:281–283. https://doi.org/10.18940/kazan.37.5_281

Imura R (1994) Geology of Kirhishima Volcano. Bull Earthq Res Inst Univ Tokyo 69:189–209. https://doi.org/10.18940/kazan.37.5_281

Imura R, Kobayashi T (1991) Eruptions of Shinmoedake Volcano, Kirishima Volcano Group, in the last 300 years. Bull Volcanol Soc Jpn 36:135–148. https://doi.org/10.18940/kazan.36.2_135

Imura R, Kobayashi T (2001) Geological map of Kirishima volcano. Geological survey of Japan, Tsukuba, Japan

Iverson RM, Dzurisin D, Gardner CA, Gerlach TM, LaHusen RG, Lisowski M, Major JJ, Malone SD, Messerich JA, Moran SC, Pallister JS, Qamar AI, Schilling SP, Vallance JW (2006) Dynamics of seismogenic volcanic extrusion at Mount St Helens in 2004–05. Nature 444:439–443

JMA (2013) National Catalogue of the Active Volcanoes in Japan (The fourth edition) III, JMA, Tokyo

JMA (2017a) Volcanic activities of Kirishima during 2017. https://www.data.jma.go.jp/svd/vois/data/tokyo/STOCK/monthly_v-act_doc/fukuoka/2017y/505_17y.pdf. Accessed 16 July 2022

JMA (2017b) Volcanic activities of Kirishima September–October 17, 2017. https://www.data.jma.go.jp/svd/vois/data/tokyo/STOCK/kaisetsu/CCPVE/shiryo/kakudai171019/2_jma.pdf. Accessed 20 March 2023

JMA (2018a) Volcanic activities of Kirishima during 2018. https://www.data.jma.go.jp/svd/vois/data/tokyo/STOCK/monthly_v-act_doc/fukuoka/2018y/505_18y.pdf. Accessed 16 July 2022

JMA (2018b) Volcanic activity report of Kirishima (Shinmoe-dake) on March 6, 2018. https://www.data.jma.go.jp/svd/vois/data/tokyo/STOCK/monthly_v-act_doc/fukuoka/18m03/201803062200_551.pdf Accessed 20 March 2023

JMA (2018c) Report for Coordinating Committee for Prediction of Volcanic Eruptions 140:97–99. https://www.https://www.data.jma.go.jp/svd/vois/data/tokyo/STOCK/kaisetsu/CCPVE/shiryo/140/140_01-2.pdf Accessed 22 July 2023

Kagiyama T, Utada H, Uyeshima M, Masutani F, Kanda W, Tanaka Y, Masuda H, Murakami H, Shiozaki I, Ichiki M, Yukutake T, Mogi T, Amita K, Oshiman N, Mishina M (1996) Resistivity structure of the central and the southeastern part of Kirishima Volcanoes. Bull Volcanol Soc Jpn 41:215–225

Kagiyama T, Utada H, Mikada H, Tsutsui T, Masutani F (1997) Structure of the Kirishima volcanic region and its magma supply system. Bull Volcanol Soc Jpn S158:S157-165

Kato K, Yamasato H (2013) The 2011 eruptive activity of Shinmoedake volcano, Kirishimayama, Kyushu, Japan-Overview of activity and Volcanic Alert Level of the Japan Meteorological Agency-. Earth Planets Space 65:489–504. https://doi.org/10.5047/eps.2013.05.009

Kobayashi T, Tobita M, Imakiire T, Suzuki A, Noguchi Y, Ishihara M (2011) Estimate of crustal deformation and pressure sources of Mt. Kirishima (Shinmoe-dake) volcanic activity, derived from InSAR analysis using Daichi SAR data. Report of Geospatial Information Authority of Japan, 121: 195-201. https://www.gsi.go.jp/common/000062664.pdf. Accessed 16 July 2022

Kozono T, Ueda H, Ozawa T, Koyaguchi T, Fujita E, Tomiya A, Suzuki YJ (2013) Magma discharge variations during the 2011 eruptions of Shinmoe-dake volcano, Japan, revealed by geodetic and satellite observations. Bull Volcanol 75:695. https://doi.org/10.1007/s00445-013-0695-4

Kozono T, Koyaguchi T, Ueda H, Ozawa T, Yamasaki T (2023) Constraints on magma storage conditions based on geodetic volume change and erupted magma volume and application to the 2011 and 2018 eruptions at Kirishima Shinmoe-dake volcano, Japan. Earth Planets Space 75:100. https://doi.org/10.1186/s40623-023-01851-2

Kurihara R, Kato A (2022) Deep low-frequency earthquake activity associated with the 2018 eruptions in the Kirishima volcanic complex Japan. Earth Planets Space 74:174. https://doi.org/10.1186/s40623-022-01723-1

Kurihara R, Obara K, Takeo A, Tanaka Y (2019) Deep low-frequency earthquakes associated with the eruptions of Shinmoe-dake in KirishimaVolcanoes. J Geophys Res Solid Earth 124:13079–13095. https://doi.org/10.1029/2019JB018032

Kyushu-University (2018) . Vertical deformation of Kirishima and Ioyama revealed by precise leveling. Report for Coordinating Committee for Prediction of Volcanic Eruptions 142:97–99. https://www.data.jma.go.jp/svd/vois/data/tokyo/STOCK/kaisetsu/CCPVE/shiryo/142/142_01.pdf Accessed 31 Mar 2023

Lees JM, Bolton EW (1998), Pressure cookers as volcano analogues. EOS Trans Am Geophys Un, edited, p620, American Geophysical Union, San Francisco, Calif

Ichihara *et al. Earth, Planets and Space* (2023) 75:144

Page 20 of 21

Lesage P, Mora MM, Alvarado GE, Pacheco J, Metaxian J-P (2006) Complex behavior and source model of the tremor at Arenal volcano, Costa Rica. J Volcanol Geotherm Res 157:49–59

Lyons JJ, Ichihara M, Kurokawa A, Lees JM (2013) Switching between seismic and seismo-acoustic harmonic tremor simulated in the laboratory: Insights into the role of open degassing channels and magma viscosity. J Geophys Res 118:277–289. https://doi.org/10.1002/jgrb.50067

Maeno F, Nagai M, Nakada S, Burden RE, Engwell S, Suzuki Y, Kaneko T (2014) Constraining tephra dispersion and deposition from three subplinian explosions in 2011 at Shinmoedake volcano, Kyushu Japan. Bull Volcanol 76:823. https://doi.org/10.1007/s00445-014-0823-9

Matsumoto K, Geshi N (2021) Shallow crystallization of eruptive magma inferred from volcanic ash microtextures: a case study of the 2018 eruption of Shinmoedake volcano Japan. Bull Volcanol 83:31. https://doi.org/10.1007/s00445-021-01451-6

Miyabuchi Y, Hanada D, Niimi H, Kobayashi T (2013) Stratigraphy, grain-size and component characteristics of the 2011 Shinmoedake eruption deposits, Kirishima Volcano, Japan. J Volcanol Geotherm Res 258:31–46. https://doi.org/10.1016/j.jvolgeores.2013.03.027

Moran SC, Malone SD, Qamar AI, Thelen WA, Wright AK, Caplan-Auerbach J (2008) Seismicity associated with renewed dome building at Mount St. Helens, 2004–2005. US Geol Surv Prof Pap 1750:27–60

Muramatsu D, Matsushima T, Ichihara M (2021) Reconstructing surface eruptive sequence of 2018 small phreatic eruption of Iwo-yama volcano, Kirishima Volcanic Complex, Japan, by infrasound cross-correlation analysis. Earth Planets Space 73:1–10.

Muramatsu D, Ichihara M, Matsushima T, Kuwano O, Tajima Y (2022) Surface eruptive dynamics of 2018 small phreatic eruption of iwo-yama volcano, japan: Constraints from seismo-acoustic observation and mud suspension rheology. J Volcanol Geotherm Res 421:107452. https://doi.org/10.1016/j.jvolgeores.2021.107452

Nagaoka Y (2020) Study on seismic velocity structure beneath active volcanoes by seismic interferometry. PhD thesis, Univ Tokyo

Nakada S, Ukawa M, Newhall CG, McNutt SR, Wright TL, Ichihara M, Geshi N (2013a) Preface, Shinmoe-dake Eruption in 2011 - An example of Less-Frequent Magmatic Activity-. Earth Planets Space 65:473. https://doi.org/10.5047/eps.2013.06.002

Nakada S, Nagai M, Kaneko T, Nagai M, Kaneko T, Suzuki Y, Maeno F (2013b) The outline of the 2011 eruption at Shinmoe-dake (Kirishima), Japan. Earth Planets Space 65:475–488. https://doi.org/10.5047/eps.2013.03.016

Nakao S, Morita Y, Yakiwara H et al (2013) Volume change of the magma reservoir relating to the 2011 Kirishima Shinmoe-dake eruption-charging, discharging and recharging process inferred from GPS measurements. Earth Planets Space 65:505–515. https://doi.org/10.5047/eps.2013.05.017

NIED (2018a) SAR observation of lava growth in the summit crater of Shinmoe-dake. Report of Coordination Committee for Prediction of Volcanic Eruption, 141, 159-163. https://www.data.jma.go.jp/svd/vois/data/tokyo/STOCK/kaisetsu/CCPVE/shiryo/141/141_01-2.pdf. Accessed 16 July 2022

NIED (2018b) Report for Coordinating Committee for Prediction of Volcanic Eruptions 140:106–107. https://www.https://www.data.jma.go.jp/svd/vois/data/tokyo/STOCK/kaisetsu/CCPVE/shiryo/140/140_01-2.pdf Accessed 22 July 2023

Nishida K, Mizutani Y, Ichihara M, Aoki Y (2020) Time-lapse monitoring of seismic velocity associated with 2011 Shinmoe-dake eruption using seismic interferometry: an extended Kalman filter approach. J Geophys Res Solid Earth 125:1–23. https://doi.org/10.1029/2020JB020180

Oikawa T, Tsutsui M, Daigaku Y, Itoh J (2012) Eruption history of Shinmoedake of Kirishima volcanoes in edo period, based on the historical documents. Bull Volcanol Soc Jpn 57:199–218. https://doi.org/10.18940/kazan.57.4_199

Ohba T, Yaguchi M, Tsunogai U et al (2021) Behavior of magmatic components in fumarolic gases related to the 2018 phreatic eruption at Ebinokogen Ioyama volcano, Kirishima Volcanic Group, Kyushu Japan. Earth Planets Space 73:81. https://doi.org/10.1186/s40623-021-01405-4

Ozawa T, Kozono T (2013) Temporal variation of the Shinmoe-dake crater in the 2011 eruption revealed by spaceborne SAR observations. Earth Planets Space 65:527–537. https://doi.org/10.1186/s40623-021-01405-4

Pallister JS, Cashman KV, Hagstrum JT, Beeler NM, Morgan SC, Denlinger RP (2013) Faulting within the Mount St. Helens conduit and implications for volcanic earthquakes. GSA Bull 125:359–376. https://doi.org/10.1130/B30716.1

Rust AC, Balmforth NJ, Mandre S (2008) The feasibility of generating low-frequency volcano seismicity by flow through a deformable channel. Geol Soc Lond Special Publ 307:45–56. https://doi.org/10.1144/sp307.4

Saito G, Oikawa T, Ishizuka O (2023) Magma ascent and degassing processes of the 2011 and 2017–18 eruptions of Shinmoedake in Kirishima volcano group, Japan, based on petrological characteristics and volatile content of magmas. Earth Planets Space 75:89. https://doi.org/10.1186/s40623-023-01836-1

Suzuki Y, Nagai M, Maeno F, Yasuda A et al (2013a) Precursory activity and evolution of the 2011 eruption of Shinmoe-dake in Kirishima volcano-insights from ash samples. Earth Planets Space 65:591–607. https://doi.org/10.5047/eps.2013.02.004

Suzuki Y, Yasuda A, Hokanishi N et al (2013b) Syneruptive deep magma transfer and shallow magma remobilization during the 2011 eruption of Shinmoe- dake, Japan-constraints from melt inclusions and phase equilibria experiments. J Volcanol Geotherm Res 257:184–204. https://doi.org/10.1016/j.jvolgeores.2013.03.017

Takeo M (2020) Harmonic tremor model during the 2011 Shinmoe-dake eruption, Japan. Geophys J Int 224:2100–2120. https://doi.org/10.1093/gji/ggaa477

Takeo M, Maehara Y, Ichihara M, Ohminato T, Kamata R, Oikawa J (2013) Ground deformation cycles in a magma-effusive stage, and sub-Plinian and Vulcanian eruptions at Kirishima volcanoes, Japan. J Geophs Res Solid-Earth 118:4758–4773. https://doi.org/10.1002/jgrb.50278

Tajima Y (2021) Estimating the ashfall volume for a small eruption using ellipse-approximated isopach analysis: how many seeking points are required to determine a suitable axis? Earth Planets Space 73:156. https://doi.org/10.1186/s40623-021-01483-4

Tajima Y, Hayashi S, Yasuda A, Itoh H (2013) Tephrostratigraphy and eruptive history of Shinmoedake volcano of the Kirishima volcanoes, Kyushu, Japan. Q Res 52:151–171. https://doi.org/10.4116/jaqua.52.151

Tajima Y, Matsuo Y, Shoji T, Kobayashi T (2014) Eruptive history of Ebinokogen volcanic area of Kirishima volcanoes for the past 15,000 years in Kyushu, Japan. Bull Volcanol Soc Jpn 59:55–75. https://doi.org/10.18940/kazan.59.2_55

Tajima Y, Nakada S, Maeno F, Huruzono T, Takahashi M, Inamura A, Matsushima T, Nagai M, Funasaki J (2020) Shallow magmatic hydrothermal eruption in April 2018 on Ebinokogen Ioyama Volcano in Kirishima Volcano Group, Kyushu Japan. Geosciences 10:183. https://doi.org/10.3390/geosciences10050183

Tajima Y, Oikawa J, Kobayashi T, Yasuda A (2022) Middle to long-term magma producing activities and the plumbing system of Shinmoedake, Kirishima Volcano: Toward a unified understanding based on volcanic products analyses and geophysical observations. Bull Volcanol Soc Jpn 67:45–68. https://doi.org/10.18942/kazan.67.1.45

Tsukamoto K, Aizawa K, Chiba K, Kanda W, Uyeshima M, Koyama T, Utsugi M, Seki K, Kishita T (2022) Three-dimensional resistivity structure of Iwo-Yama Volcano, Kirishima Volcanic Complex, Japan: Relationship to shallow seismicity, surface uplift, and a small phreatic eruption. Geophys Res Lett 45:12821–12828. https://doi.org/10.1029/2018GL080202

Ueda H, Kozono T, Fujita E et al (2013) Crustal deformation associated with the 2011 Shinmoe-dake eruption as observed by tiltmeters and GPS. Earth Planet Space 65:517–525. https://doi.org/10.5047/eps.2013.03.001

Utada H, Kagiyama T, EM Research Group for Kirishima Volcano (1994) Deep resistivity structure of Kirishima Volcano (I). Bull Earthq Res Inst Univ Tokyo 69:241–255

White RA, McCausland WA (2019) A process-based model of pre-eruption seismicity patterns and its use for eruption forecasting at dormant stratovolcanoes. J Volcanol Geotherm Res 382:267–297. https://doi.org/10.1016/j.jvolgeores.2019.03.004

Yamada T, Ueda H, Mori T, Tanada T (2019) Tracing volcanic activity chronology from a multiparameter dataset at Shinmoedake volcano (Kirishima), Japan. J Disaster Res 14:687–700

Yamamoto K, Ida Y (1994) Three-dimensional P-wave velocity structure of Kirishima volcanoes using regional seismic events. Bull Earthq Res Inst Univ Tokyo 69:267–289

Yamamoto K, Ida Y (1997) Significant P wave attenuation for a specific frequency range beneath Kirishima Volcano, Japan. Geophys Res Lett 24:1275–1278. https://doi.org/10.1029/97GL01157

Yamazaki K, Yamashita Y, Komatsu S (2020) Vault-housed extensometers recorded a rapid initial pulse before precursory magma reservoir inflation related to the 2011 eruption of Shinmoe-dake, Japan. Earth Planets Space 72:83. https://doi.org/10.1186/s40623-020-01211-4

Yukutake Y, Kim A, Ohminato T (2023) Estimation of volcanic earthquakes at Kirishima Volcano using machine learning. Authorea. https://doi.org/10.22541/essoar.168056823.39656162/v1

Publisher's Note